

Buckling and Post Buckling Analysis of CFRP Laminated Panel under Uniaxial Compressive Loading

-Muhammad Shuaib N K-

A Dissertation Submitted to
Indian Institute of Technology Hyderabad
In Partial Fulfillment of the Requirements for
The Degree of Master of Technology/ Doctor of Philosophy



भारतीय प्रौद्योगिकी संस्थान हैदराबाद
Indian Institute of Technology Hyderabad

Department of Mechanical and Aerospace Engineering

June, 2016

Acknowledgements

I would like to express my hearty gratitude to the Department of Mechanical and Aerospace Engineering, IIT Hyderabad, for the provision of facilities and opportunities that nurtured me to be what I am.

I extend my sincere gratitude and thankfulness towards my project advisors Dr. M. Ramji and Dr. Gangadharan Raju, for their valuable guidance and continuous encouragement.

I would like to use this opportunity to express my gratitude to all the Department faculty members for their help and support. I also would like to thank the unceasing encouragement from my parents.

I am also indebted towards the help and support provided by the Optics lab members, Central workshop, and all of my friends.

I also place on record my thankfulness to each and every one who directly or indirectly lent their time and effort for this venture.

Dedication


Dedicated to family, teachers and friends

Abstract

An experimental study has been carried out to investigate the buckling and post-buckling behavior of Carbon fibre reinforced polymer (CFRP) composite flat panel with and without hole. For the experimental study, panels were manufactured using hand-layup followed by vacuum bagging process. An appropriate fixture has been conceived and developed for realizing the simply supported boundary condition on all the edges and providing uniform compressive loading. The composite panels were then subjected to uniaxial compression loading using the MTS machine and the plates were simply supported on all the sides using specially designed fixture. Digital Image Correlation technique (DIC) is used for capturing whole field strain, axial displacement, out of plane deflection and mode shapes. Experimental buckling and post-buckling results are then compared with the finite element analysis for validation. A comparison study between plate with and without hole with respect to their buckling behaviour has also been carried out. Failure mechanism from the experiment has also been captured.

Declaration

I declare that this written submission represents my ideas in my own words, and where others' ideas or words have been included, I have adequately cited and referenced the original sources. I also declare that I have adhered to all principles of academic honesty and integrity and have not misrepresented or fabricated or falsified any idea/data/fact/source in my submission. I understand that any violation of the above will be a cause for disciplinary action by the Institute and can also evoke penal action from the sources that have thus not been properly cited, or from whom proper permission has not been taken when needed.



(Signature)

MUHAMMAD SHWAB N.K

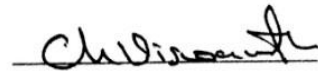
(- Student Name -)

ME11B15M000008

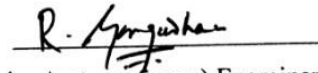
(Roll No)

Approval Sheet


This thesis entitled Buckling and Post Buckling Analysis of CFRP Laminated Panel under Uniaxial Compressive Loading by Muhammad Shuaib N K is approved for the degree of Master of Technology from IIT Hyderabad.



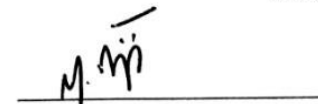
(Dr. Viswanath Chinthapenta, Asst. professor) Examiner
Dept. of Mechanical and aerospace engineering
IITH



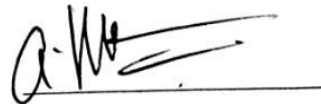
(Dr. Gangadharan Raju, Asst. professor) Examiner
Dept. of Mechanical and aerospace engineering
IITH



(Dr. Syed Nizamuddin Khaderi, Asst. professor) Examiner
Dept. of Mechanical and aerospace engineering
IITH



(Dr. M. Ramji, Asso. professor) Adviser
Dept. of Mechanical and aerospace engineering
IITH



(Dr. G. Prabusankar, Asso. professor) Chairman
Dept. of Chemistry
IITH

Contents

Declaration.....	Error! Bookmark not defined.
Approval Sheet	Error! Bookmark not defined.
Acknowledgements.....	ii
Abstract.....	iv
1 Introduction and literature review	1
1.1 Introduction.....	1
1.1.1 Introduction to plate buckling	2
1.1.2 Importance of buckling	4
1.2 Literature review.....	4
1.3 Scope and objective	7
1.4 Theoretical formulation	8
1.5 Thesis layout.....	10
2 Finite element analysis.....	11
2.1 Introduction.....	11
2.2 Geometry and material properties.....	12
2.2.1 Geometry and problem description	12
2.2.2 Material properties	13
2.3 FEA modelling of buckling	14
2.3.1 FEA model description.....	14
2.3.2 Eigen buckling.....	14
2.3.3 Post buckling analysis	15
2.4 Result and conclusion	15
2.4.1 Layup optimization.....	15
2.4.2 Mode shapes.....	18

2.4.3	Hole size study	19
2.4.4	Post buckling results.....	20
2.5	Closure	21
3	Experimental studies.....	23
3.1	Introduction.....	23
3.2	Material characterisation.....	23
3.2.1	Specimen geometry and fabrication	24
3.2.2	Test results are material properties.....	24
3.2.3	Burn off test result.....	26
3.3	Experimental buckling study	27
3.3.1	Panel fabrication.....	27
3.3.2	Fixture design and fabrication.....	29
3.3.3	Experimental setup	30
3.3.4	Post processing	31
3.4	Result and discussion.....	31
3.4.1	Mode shapes.....	34
3.4.2	Axial and out-of-plane deflection.....	36
3.4.3	Failure mechanism	43
3.5	Closure	45
4	Conclusion and recommendation for future work.....	47
4.1	Conclusion	47
4.2	Recommendation for future work.....	48
References	49

List of Figures

1.1	Benefits of B787 over B767 and insights.....	2
1.2	Carbon fiber usage in different industries over years.....	2
1.3	Typical simply supported plate buckling mode.....	3
1.4	Buckling behaviour of simply supported plate.....	4
1.5	Simply supported plate under uniaxial compressive loading.....	8
2.1	Geometry and node positions of shell and solid elements.....	12
2.2	Geometry, loading and boundary conditions of plate without hole.....	12
2.3	Geometry, loading and boundary conditions of plate with hole.....	13
2.4	Finite element model of buckling specimens.....	14
2.5	Load v/s out-of-plane and axial deflection for different lay-up sequences.....	16
2.6	Load v/s end shortening graph for various quasi isotropic lay-up sequences.....	17
2.7	Mode shapes of CFRP composites from FEA.....	18
2.8	Different mode shapes for buckling of quasi-isotropic panel from FEA.....	19
2.9	1 st buckling mode shapes of quasi-isotropic panel from FEA.....	19
2.10	Pre-buckling and post buckling behaviour from non-linear buckling analysis.....	20
2.11	Pre-buckling and post buckling behaviour of panel with and without hole.....	21
3.1	Specimen geometry for CFRP composite material characterisation.....	24
3.2	Experimental material characterisation tests to extract material properties.....	25
3.3	Panel fabrication using hand lay-up and vacuum bagging technique.....	28
3.4	Fabricated 16 layered CFRP composite panels.....	28
3.5	Fixture for simply supported boundary condition for buckling experiment.....	29
3.6	Experimental setup for buckling test of composite flat panels.....	30
3.7	Speckled image of the panel captured by CCD camera.....	31

3.8	Finite element (FEA) and experimental (DIC) comparison of in plane axial displacement of 16 layered CFRP panel.....	32
3.9	Cross sectional view of bottom ‘V’ groove with panel.....	33
3.10	Axial displacement contour with axial displacement extracting lines.....	33
3.11	Finite element (FEA) and experimental (DIC) comparison of out-of-plane deflection of 8 layered UD specimen.....	34
3.12	FEA and experimental (DIC) comparison of out-of-plane deflection of 8 layered quasi isotropic specimen.....	34
3.13	Finite element (FEA) and experimental (DIC) comparison of out-of-plane deflection of 16 layered UD specimen.....	35
3.14	FEA and experimental (DIC) comparison of out-of-plane deflection of 16 layered quasi isotropic specimen.....	35
3.15	FEA and experimental (DIC) comparison of out-of-plane deflection of 16 layered quasi isotropic panel with 30mm hole.....	36
3.16	Experimental (DIC) and finite element (FEA) comparison of end shortening of quasi-isotropic lay-up	37
3.17	Experimental (DIC) and finite element (FEA) comparison of variation of out of plane deflection with loading.....	38
3.18	Experimental (DIC) and finite element (FEA) comparison of variation of in-plane axial displacement with loading for 16 layered panel.....	40
3.19	Experimental (DIC) and finite element (FEA) comparison of variation of out of plane deflection with loading for 16 layered panel.....	40
3.20	Experimental (DIC) and finite element (FEA) comparison for 16 layered quasi isotropic plate with hole.....	41
3.21	Experimental in-plane and out-of-plane displacement for quasi isotropic panel...	42
3.10	Filure propagation of quasi isotropic panel from DIC.....	43
3.10	Critical regions of failure for quasi isotropic plate without hole.....	44
3.10	Critical regions of failure for quasi isotropic plate with hole	45

List of tables

2.1	CFRP material properties.....	13
2.2	Lay-up sequences and corresponding critical buckling load.....	16
3.1	Properties obtained from material characterisation.....	26
3.2	Properties obtained from burn off test.....	27

Chapter 1

Introduction and literature review

1.1 Introduction

Composite materials have a wide range of applications because of its high strength/stiffness to weight ratio, excellent fatigue and tailor-ability properties. Starting from traditional application areas such as military aircraft, now composite has grown rapidly to make an impact on various engineering and industrial fields including automobile, civil structures, sports equipment and even marine structures. As the range of application increases, it is very important to have a deep understanding of all the mechanical behaviors such as stiffness, strength and stability behavior of the composites.

A composite material consists of two or more chemically distinct constituents having a distinct interface separating them. Composite helps us to attain superior properties in our desired way, compared to the each constituent consists in the composites separately. Mostly there will be two phases for composites, matrix and reinforcement, which is usually a particulate or a fiber. In most cases reinforcing phase will be harder and stronger than matrix and provides strength and stiffness to the composite. Continues fiber composites tend to be much stronger and stiffer than particulate composites and contains more volume percentage of fiber. Matrix keeps fibers in position and provides the necessary flexibility and at the same time it protects fibers from environment.

Carbon fiber reinforced polymer (CFRP) composite is comparatively expensive to produce, although it has been extensively used in today's aircraft industry, automobile and civil structures because of its high strength, low density and higher stiffness.

Aircraft industries are able to achieve considerable amount of advantages in terms fuel efficiency, low emission and noise reduction by replacing composites in place of aluminium in different structures including primary structures namely fuselage and wing[1].

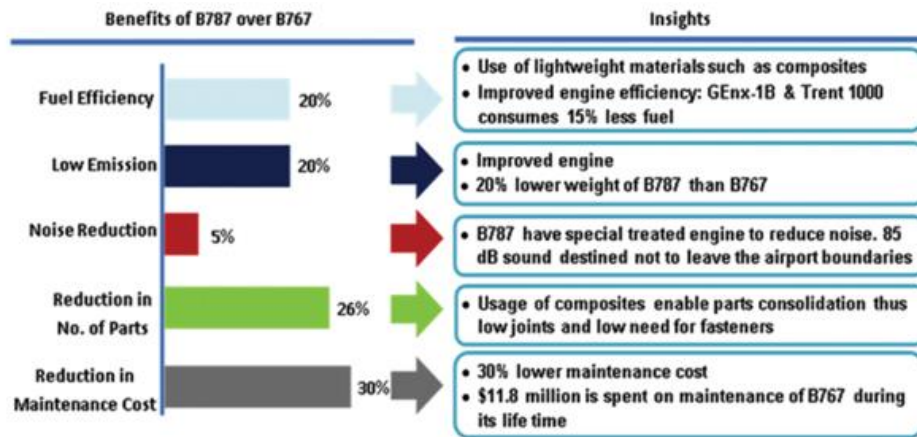


Fig 1.1: Benefits of B787 over B767 and insights [1].

Advantages of Boing 787, in which up to 50% of structures are built up of using CFRP and other composites comparing with boing 767, which has comparatively lesser composite structures are shown in Fig 1.1 [1]. The increase in usage of CFRP composites from 2010 to 2015 and expected hike by 2020 in different industries are also illustrated in Fig 1.2 [2].

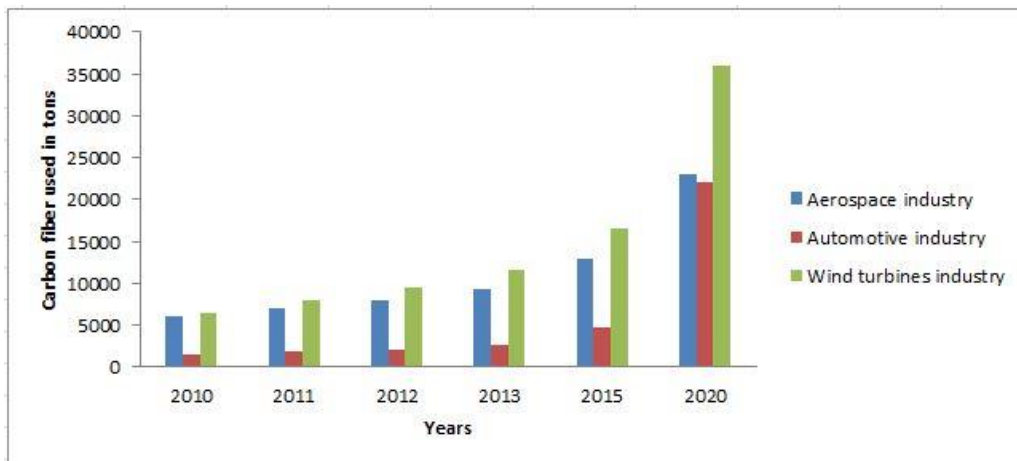


Fig 1.2: Carbon fiber usage in different industries over years [2].

1.1.1 Introduction to plate buckling

Buckling is simply the geometrical instability of a structure and characterized by sudden sideways failure of the structural member subjected to high compressive stress, where the compressive stress at the point of failure is lesser than the ultimate

compressive strength of the material. Buckling occurs due to the presence of imperfections in the geometry of the structure. When the compressive load is increasing, at a certain point further load is able to be sustained in one or two states of equilibrium such as purely compressed stage or a laterally deformed stage, which we call as buckling. When a column buckles, lateral deformation develops along the column length, whereas when a plate with all sides being simply supported buckles, the deformation transverse to the plane of the plate has a two dimensional wavy nature as shown in Fig 1.3.

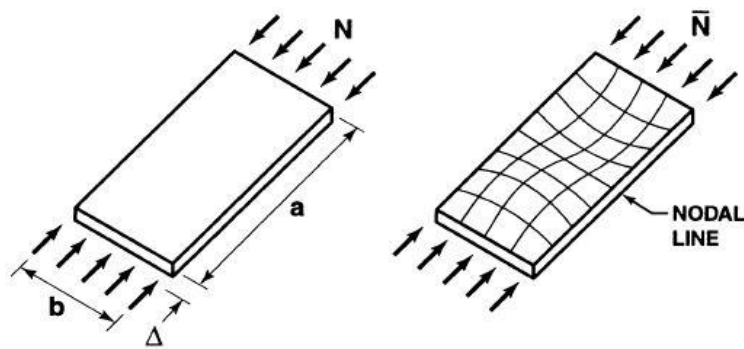


Fig 1.3: Typical simply supported plate buckling mode [27]

When the plate undergoes compressive loading, initially it shortens in the load direction while remaining flat. Then at critical buckling load, the deformation path bifurcates to buckled shape. Even after buckling, plate can support an increased load over the buckling load with a lesser stiffness, shown in the Fig 1.3.a. This is because of the side edges which are still under pure compression by the help of side supports. Most of the entire load in the post buckling region is taken by this side edges. Out-of-plane deflection behavior in the pre buckling and post buckling regime is shown in the Fig. 1.3.b.

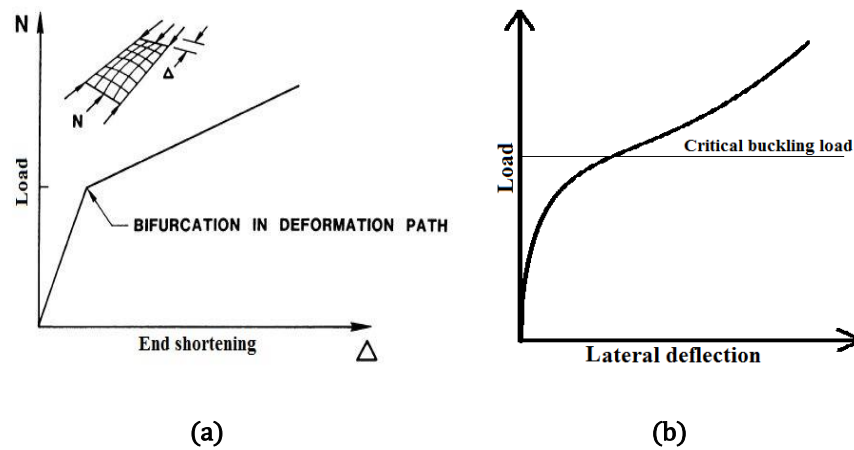


Fig 1.4 Pre buckling and post buckling behaviour of simply supported plate under compressive loading (a) End shortening (b) Out-of-plane deflection [27].

1.1.2 Importance of buckling

As the range of application of CFRP composites increases, it is very important to have a deep understanding of all the mechanical behaviors such as stiffness, strength and stability of the composites. As composites are commonly used in mass reduction applications, most of the structures are relatively thin in nature and there is a higher chance for the buckling under compressive loading. Because of this thin nature of composite structures, buckling is an important design driver for the safe and reliable design of these structures. Also the presences of cut outs are unavoidable in composite structures as cutouts are often required in structural components due to functional requirements.

1.2 Literature review

The load carrying capacity and buckling behavior of fiber composites under compression loading has been intensively considered by the researchers considering the fact that majority of the fiber composite structures are used in various applications are in the form of thin plates. There have been numerous studies done on different laminated fiber composite structures which are likely to use in Aerospace, civil, automobile, sports, biomedical and other applications. As buckling is the important design driver for the thin laminated composite plates, most of the buckling studies have been done on the thin plates with various boundary conditions.

Euler (1795) has done the initial theoretical studies of elastic buckling on the column flexural buckling and proposed the very first analytical method for predicting the buckling strength of columns. Later, in 1899 Prandtl and Michell published the first research on flexural torsional buckling of beam with rectangular cross-section and then it has extended to 'I' cross-section beams by Timoshenko.

Chia and Prabhakara [3] have studied the post buckling behavior of unsymmetrically layered rectangular anisotropic plates considering each layer having different elastic properties, arbitrary thickness and orientation with respect to the plate axes. Using multiple Fourier equations, governing differential equations are solved for clamped boundary conditions as well as simply supported edges. Later, Harris [4] has done a significant study on cross ply rectangular panel under in-plane bi-axial loading. Expression for in-plane stiffness and critical buckling load of panel immediately after buckling has been derived and then he has stated that the coupling term affects the stiffness at buckling regime because of the associated changes in buckling mode shapes.

Zhang and Mathews [5] have investigated the impact of the geometrical imperfections (assumed to be a general form of a double-sine series) on the post-buckling behavior of cylindrically curved and flat composite panels with simply supported boundary condition. Panels with different lay-ups, different curvatures and different materials are considered in their numerical studies. Later, they have done a similar study on non-bifurcational behavior of same kind of flat and curved unsymmetrically laminated composite panels under compression and shear loading [6]. Computations have been carried out for simply supported panels with different materials, different lay-ups and different curvatures and they found out that lateral deflection is involved under compressive loading for unsymmetrical cross ply laminates and under shear loading for unsymmetrical angle ply layers.

Nemath [7] has studied the importance of anisotropy on the buckling of symmetric composite panels under compressive loading. A non dimensional form of the governing differential equation has been developed. Another non dimensional parameter has been also presented to assess when one can neglect the anisotropic bending stiffnesses in buckling analysis. A finite element has been carried out by him to analyse the importance of the fiber orientation, boundary conditions, stacking sequence, aspect ratio and thickness in anisotropic bending stiffnesses.

Later, Tung and Surderas [8] investigated the buckling behavior of orthotropic rectangular panels under biaxial loading with simply supported boundary conditions. Both compression/compression and compression/tension cases are taken into account and found out the first buckling mode shape for the plate with effectively nearly square shape geometry is having single half sine wave in both direction for bi-axial compressive loading and single half wave in the tension direction for compression/tension loading. Later, Post-buckling behaviour of simply supported orthotropic rectangular panels subjected to a combined bi-axial compression and shear loading has been studied by Wang [9]. The coupled nonlinear partial differential equations are brought down to uncoupled partial

differential equations using a perturbation method. Uncoupled partial differential equations are then solved using the double Fourier series method. The influence of loading parameter and aspect ratios on the post buckling behavior are studied numerically for glass-epoxy composites. Followed by this research Tuttle and Singhatanadgid [10] have numerically studied the CFRP composite plate subjected to bi-axial loading using Galerkin method and experimentally and found out that critical buckling load is increases with increase in traverse tensile loading.

As the edge support conditions are playing a crucial role in the buckling of laminated thin composite plates, Chainarin and Singhatanadgid [11] have done a research on buckling of composite rectangular and skew plates with various boundary conditions. Numerical study has been carried out for simply supported, clamped, free edge boundary conditions and its combinations using Ritz method. Then using Kantorovich method, the out-of-plane deflection function is determined in form of hyperbolic and trigonometric functions.

Later, Cheon and Sang-Youl [12] have done a significant study on the post-buckling of laminated composite plate subjected to combined in-plane shear, compression and lateral loading. Natural strain method is used for the finite element formulation and an element based Lagrangian formulation is further used to study influence of number of layers, various types of loading and materials on the post buckling regime numerically. Zong and Chao Gu [13] investigated the influence of linearly varying in-plane load on buckling of symmetrical cross ply laminated composites panel with simply supported sides based on first order shear deformation theory.

The presence of holes in the composite panel is unavoidable as there is always a need of joining multiple structures together. Christopher and Schafer [14] have researched on the elastic buckling of thin plate with hole subjected to compression loading or bending. The finite element based parametric study has demonstrated that the holes can either increase or decrease a plate's critical buckling load and may create unique mode shapes depending up on the hole geometry and spacing. Later, Komur and Faruk Sen [15] have done a finite element study on woven glass polyester laminated composite plates with an elliptical cut out. A parametric study has performed by changing the size and position of elliptical cut out for both angle ply and cross ply laminates. The effect of rectangular cut out has been considered by Ozben and Arslan [16] for fiber reinforced thermoplastic laminated composite plates with various elastic moduli. The effect of elastic moduli and other material properties on expansion of the plastic zone and the residual stresses are also taken into consideration for laminated panels with simply supported and clamped boundary conditions. Later, Lakshmi and Krishnamohana [17] have studied on symmetrically laminated quasi

isotropic graphite/epoxy composite panels subjected to linearly varying compressive in-plane load. The effects of size and orientation of rectangular cutout, plate aspect ratio, thickness and boundary conditions are addressed using the finite element method.

Although we get the critical loads using load versus displacement behavior from experimental buckling tests, getting whole field strain and out-of-plane deflection is not possible using strain gauges, noncontact laser displacement meters [23] or using linear variable displacement transducers [24], where we get the deflection of point or multiple points. Recently developed 3-D DIC technique can be used to capture the whole field deflection behavior which provides insight into the physics behind buckling of plates. Bisagni [25] has studied the effects of minor imperfections while manufacturing and the residual thermal strains on post buckling response using strain gauges and 3-D DIC technique. Initial geometric imperfections, strain and displacements are measured using 3-D DIC. Rouran [26] has used 3-D DIC technique to determine the delamination buckling and growth behaviors of a cross-ply composite laminate. In this study 3-D DIC technique has been used to analyze pre buckling and post buckling behavior such as, whole field strain, axial displacement and out of plane deflection of composite panel.

1.3 Scope and objective

The composite structures are getting lighter and thinner constantly as it is being extensively used in many weight reduction applications. As the composite structures are mostly used in forms of relatively thin panels, its mechanical behavior against compressive loading and buckling has become more prominent in aircraft structure applications. Further, not much works exist in the domain of experimental buckling using whole field technique like DIC as it would help us understanding the overall panel behavior at the pre buckling and post buckling regime. In any mechanical applications, structures would have cut outs and holes for the functional requirements. So the effect of cutout in the composite structures is another important design driver for the safe and reliable design of these structures.

Experimental study has to be carried out for the better understanding of pre and post buckling behaviour of CFRP panel with and without holes. Whole field techniques like DIC need to be established for the full depth understanding of such studies exploring the whole field nature. Proper fixture is also needs to be conceptualized and fabricated for the better realization of all the boundary condition and loading of CFRP composite panels. Various parameters such as subset size and step size have to be optimized and evaluated for extracting the accurate results using DIC.

1.4 Theoretical formulation

Stiffness of laminated plate is obtained from stiffness of each constituent lamina, assuming that laminae are perfectly bonded together and there is no slipping in between laminae. Taking all the thin plate assumption into consideration, governing buckling differential equation for a symmetric laminated plate subjected to in-plane load has been derived using classical laminate theory [27].

$$D_{11} \frac{\partial^4 w}{\partial x^4} + 4D_{16} \frac{\partial^4 w}{\partial x^3 \partial y} + 2(D_{12} + 2D_{66}) \frac{\partial^4 w}{\partial x^2 \partial y^2} + 4D_{26} \frac{\partial^4 w}{\partial x \partial y^3} + D_{22} \frac{\partial^4 w}{\partial y^4} + N_x \frac{\partial^2 w}{\partial x^2} + 2N_{xy} \frac{\partial^2 w}{\partial x \partial y} + N_y \frac{\partial^2 w}{\partial y^2} = 0$$

Where D_{ij} is the plate bending stiffness, w is out-of-plane deflection and N is the line pressure load. Thin composite plate with all the sides are simply supported under uniaxial compressive loading is shown in the Fig 1.3.

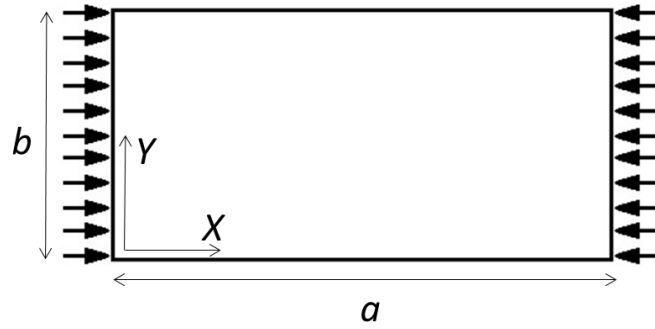


Fig 1.5: Simply supported plate under uniaxial compressive loading

For a symmetric laminate plate subjected to in-plane axial (along dir. 1) load, governing differential equation can be written as,

$$D_{11} \frac{\partial^4 w}{\partial x^4} + 4D_{16} \frac{\partial^4 w}{\partial x^3 \partial y} + 2(D_{12} + 2D_{66}) \frac{\partial^4 w}{\partial x^2 \partial y^2} + 4D_{26} \frac{\partial^4 w}{\partial x \partial y^3} + D_{22} \frac{\partial^4 w}{\partial y^4} + N_x \frac{\partial^2 w}{\partial x^2} = 0$$

When all sides are simply supported,

$$X=0,a: \delta w = 0 \text{ and } \delta M_x = -D_{11} \frac{\partial^2 w}{\partial x^2} - D_{12} \frac{\partial^2 w}{\partial y^2} - 2D_{16} \frac{\partial^2 w}{\partial x \partial y} = 0$$

$$Y=0,b: \delta w = 0 \text{ and } \delta M_y = -D_{12} \frac{\partial^2 w}{\partial x^2} - D_{22} \frac{\partial^2 w}{\partial y^2} - 2D_{26} \frac{\partial^2 w}{\partial x \partial y} = 0$$

Where M is the bending moment. The presence of D_{16} and D_{26} in the governing differential equation and boundary condition makes a closed form solution impossible. That is, lateral deflection δw , can not be separated into a function of x and y . Although an approximate Rayleigh-Ritz solution was obtained by Ashton and Waddoups by substituting the variation in lateral deflection expression

$$\delta w = \sum_{m=1}^{\infty} \sum_{n=1}^{\infty} A_{mn} \sin \frac{m\pi x}{a} \sin \frac{n\pi y}{b}$$

Where m and n are the number of half sine waves along x and y axes. Equation satisfies the geometric boundary conditions of the problem ($\delta w = 0$) on all edges, but not the natural boundary conditions ($\delta M_x = 0$) on all edges, so the result probably converge slowly towards the actual solution.

For the unidirectional laminates, where bend-twist coupling stiffness (D_{16} and D_{26}) are zero, the governing differential equation can be written as,

$$D_{11} \frac{\partial^4 w}{\partial x^4} + 2(D_{12} + 2D_{66}) \frac{\partial^4 w}{\partial x^2 \partial y^2} + D_{22} \frac{\partial^4 w}{\partial y^4} = N_x \frac{\partial^2 w}{\partial x^2}$$

The deformation transverse to the plane of plate has a two dimensional wavy nature, so the out of plane displacement (w) can be assumed as a function, shown below

$$w = \sum_{m=1}^{\infty} \left[\sum_{n=1}^{\infty} \left(a_{mn} \sin \frac{m\pi x}{a} \sin \frac{n\pi y}{b} \right) \right]$$

Where p , q are number of half sine waves along x and y axes respectively. From equation (1) and (2), the critical buckling load can be expressed as,

$$N_x = \frac{\pi^2 [D_{11} m^4 + 2(D_{12} + 2D_{66}) m^2 n^2 R^2 + D_{22} n^4 R^4]}{a^2 m^2}$$

Where R is the aspect ratio (a/b). For the unidirectional plate of aspect ratio 2 and with all the sides are simply supported under uniaxial compressive loading, critical buckling load can be re-written as,

$$N_x = \frac{\pi^2 [D_{11} + 8(D_{12} + 2D_{66}) + D_{22}]}{a^2}$$

1.5 Thesis layout

In chapter 1, basics and applications of composites followed by the importance of buckling on composite structures have been discussed. Brief literature review has been presented on buckling of flat panel under various loading and boundary conditions, cut outs and DIC. Importance of whole field techniques like DIC has also established. Scope and objective of the present work is also defined at the end of the chapter.

Chapter 2 covers the finite element study on the CFRP flat panel with all edges with simply supported boundary condition being subjected to in-plane uniaxial compressive loading. Further it also includes an optimization study on lay-up sequence toward higher buckling load and stiffness. Based on this optimization study, suitable lay-up sequence is suggested for the experimental work. Influence of hole size on buckling behavior is also analysed.

Chapter 3 described the experimental study on 8 and 16 layered CFRP panels having pure unidirectional (UD) and quasi-isotropic lay-up sequences using 3-D DIC technique. Experimental material characterisation of CFRP laminates is also included for the completeness. In the end experimental results are compared with FEA predicated results for validation.

Chapter 4 includes the conclusion and recommendation of the future works related to the buckling study of the CFRP panel.

Chapter 2

Finite element analysis

2.1 Introduction

Finite element study has been carried out using commercial finite element software Ansys version 15.0. An 8 noded shell element (Shell-281) [28] having 6 degree of freedom per node is chosen for performing the buckling and post-buckling analysis of composite panels. Shell elements are typically planar element, used to model structures where thickness is negligible compared to its length and width and which experience large bending. Comparing to solid elements which provides similar result, the shell elements has great advantage in saving the computational effort and time. The geometry of shell281 and solid186 are shown in Fig 2.1. Comparing to other shell elements, shell281 is used for analyzing moderately thick shell structures and well suited for large rotation and large strain nonlinear applications. The six degree of freedom on each node includes three translations along x, y, z axes and three rotations about x, y, z axes. The exactness in modeling composite shells is governed by the first order shear deformation theory which is commonly referred to as Mindlin-Reissner shell theory [29].

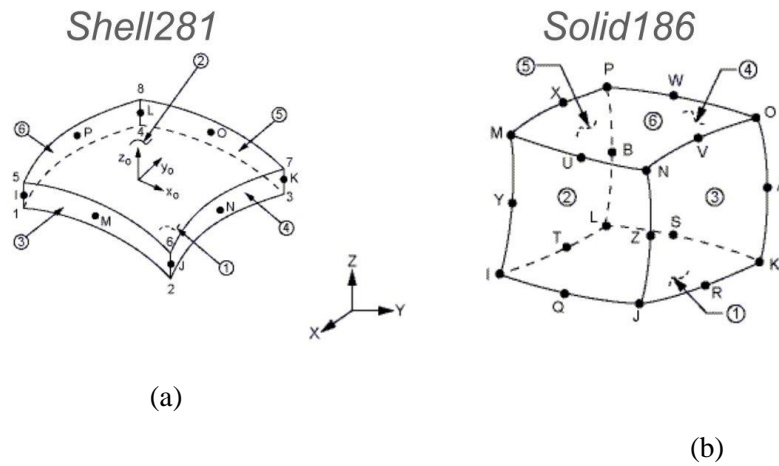


Fig 2.1: Geometry and node positions of (a) shell281 element (b) solid186 element [28]

2.2 Geometry and material properties

Geometry of the FEA model, boundary condition, loading and material properties used in finite element modelling are described in this section.

2.2.1 Geometry and problem description

Finite element and experimental studies are carried out for an 8 layered and 16 layered Carbon fiber reinforced polymer composite (CFRP) rectangular flat plate with and without hole, having a dimensions of Length (a) = 400 mm, Width (b) = 200 mm. Thickness (t) of the plate is 1.8mm for 8 layered panel and 3.5mm for 16 layered panel. The plate is analysed for in-plane uniaxial compressive loading and the boundary conditions are shown in the Fig 2.2. All the sides are simply supported and along with that, axial displacement is constrained at $u = 0$. Both the corner nodes at $v = 0$ is constrained along transverse direction to restrict the plate from moving along v direction. Plate with various lay-up sequences has been studied under these boundary conditions.

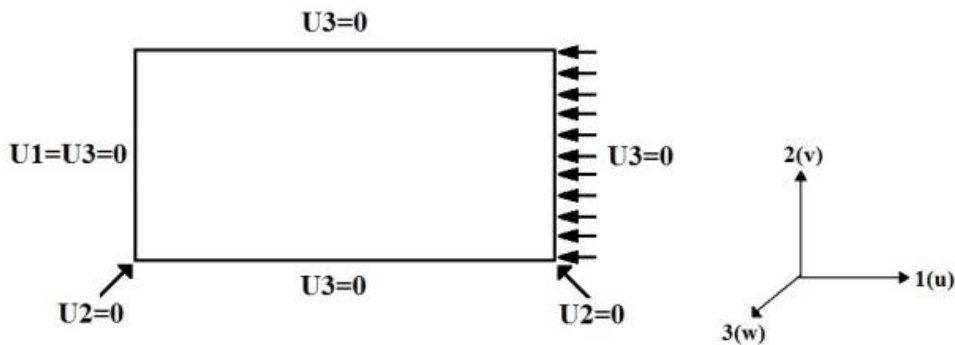


Fig 2.2 Geometry, loading and boundary conditions of plate without hole

Similar boundary conditions and loading have been used to study the effect of introducing a hole in the panel. Finite element study of plate with hole has been done with different hole size to study its impact on the buckling behaviour. Geometry, loading and boundary condition of the panel after introducing hole has been given in the Fig 2.3

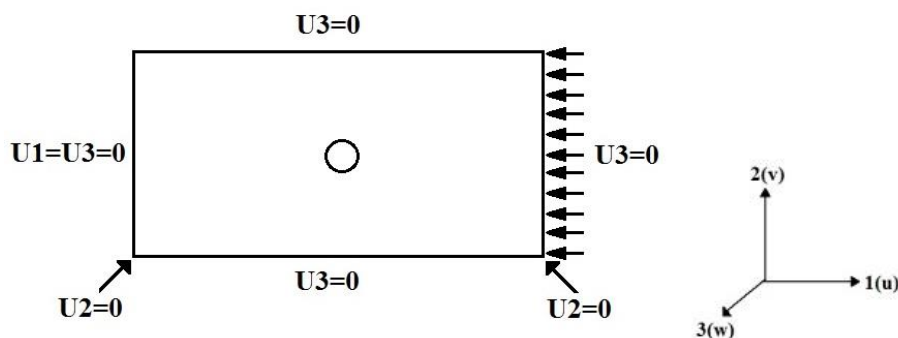


Fig 2.3 Geometry, loading and boundary conditions of plate with hole

2.2.2 Material properties

Material properties of CFRP composite laminates has been obtained from material characterisation test (discussed in section 3.2), and given as the input for the FE simulation to ensure the appropriate correlation with the experimental results. For the current experimental study unidirectional Carbon fiber mat having a density of 200 grams per square meter is used as the reinforcement and CY-230 epoxy resin mixed with HY-951 hardener in a weight-ratio of 10:1 is used as the matrix for fabricating CFRP panels using vacuum bagging. The elastic properties obtained from material characterisation are listed below.

Table 2.1: CFRP material properties

Material properties		Value
Longitudinal Modulus	E_{11}	98.41 GPa
Transverse modulus	E_{22}	6.3 GPa
In-plane shear modulus	G_{12}	1.53 GPa
Out-plane shear modulus	G_{23}	1.91 GPa
In-plane Poisson's ratio	ν_{12}	0.23
Out-plane Poisson's ratio	ν_{23}	0.30

2.3 FEA modelling of buckling

Finite element analysis is a fine and powerful computational tool for Eigen buckling analysis as well as post buckling analysis. In present study, commercial FEA software, Ansys 15.0 has been used for pre/post buckling analysis of CFRP panel with and without hole as well as failure prediction.

2.3.1 FEA model description

The meshed model of both plate with hole and without hole modeled in Ansys 15.0 as per the problem dimensions described in section 2.2.1 is given in the Fig 2.4. For the panel without hole, element size is chosen to be 10mm x 10mm, with a total number of 800 elements over the complete plate of dimension 200mm x 400mm after a mesh convergence study. For the plate with hole, a fine meshing has been done with 48 elements around the circumference of the hole for better results and is obtained from detailed mesh convergence study.

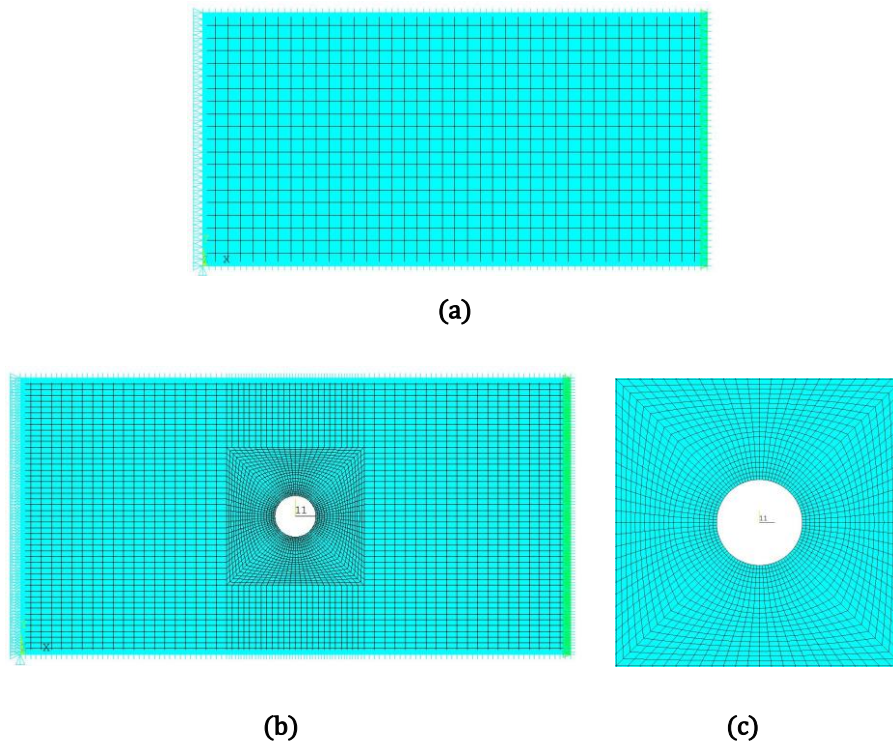


Fig 2.4: Finite element model of buckling specimen (a) panel without hole (b) panel with hole (c) zoomed view of meshing around the hole.

2.3.2 Eigen buckling

Linear buckling is the most basic form of buckling analysis in FEA. Eigen value buckling analysis predicts the theoretical buckling strength of an ideal linear elastic structure. Buckling loads are derived from structural Eigen values computed from boundary

conditions and loading. In each element, a small displacement of a perturbed shape is assumed which includes a stress dependent stiffening effect and adds to the linear static stiffness. Subtracting stress independent stiffness from the linear static stiffness term later causes buckling. Eigenvalue buckling problem extracts the load at which the model stiffness matrix becomes singular. A base of the ideal structure with a preload is taken and Block Lanczos mode extraction method was used to compute the critical buckling load of the composite plates. Eigen buckling analysis also predicts the mode shape for corresponding critical buckling loads.

2.3.3 Post buckling analysis

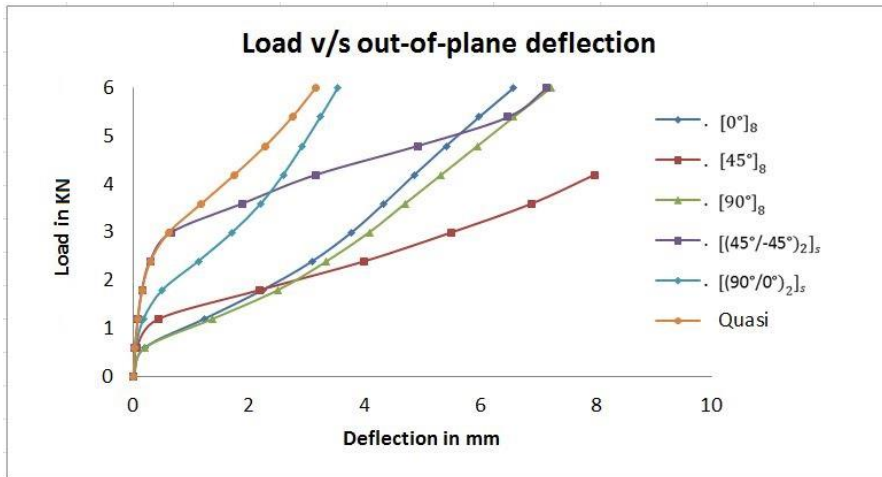
Nonlinear post-buckling analysis is carried out on the composite panels to study the reduction of stiffness of the plate after buckling and also the out of plane displacement behaviour of the panels. An initial imperfection in geometry or a small lateral load is necessary to initiate the instability of the structure which leads to buckling. The first mode shape from Eigen buckling analysis has been used as the initial imperfection with a scaling factor of 10% of the thickness of the plate. In the post-buckling regime, the strain displacement relationship is nonlinear and requires nonlinear solvers to solve the resulting finite element matrix equations. Newton-Raphson method with automatic load stepping option was chosen to perform the post-buckling analysis. In-plane displacement, out-of-plane deflection and stress distributions at each load step over the complete plate can be obtained from non-linear post buckling analysis.

2.4 Result and conclusion

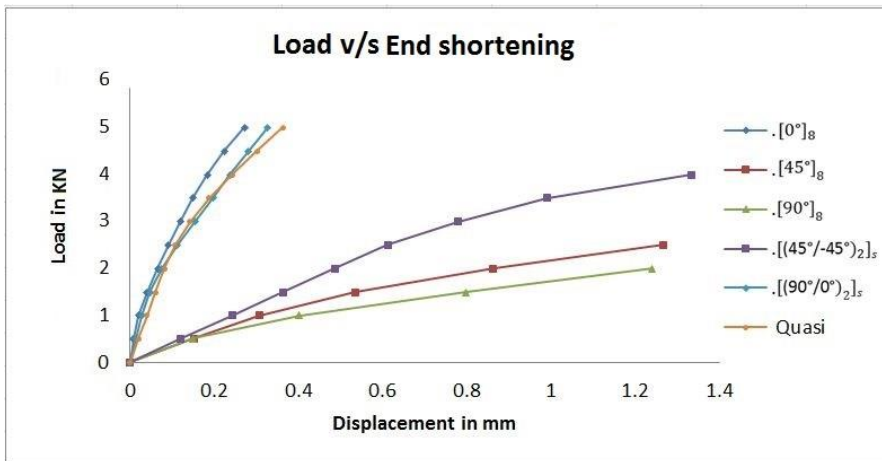
The FEA results obtained from Eigen buckling and post buckling analysis are discussed in this section.

2.4.1 Layup optimization

Buckling behavior of 8 layered CFRP composite panels having different lay-up sequences are studied in detail. Load v/s in plane displacement and out-of-plane deflection for different lay-ups are given in Fig 2.4 and corresponding critical buckling load is given in table 2.2.



(a)



(b)

Fig 2.5: Load v/s out-of-plane and axial deflection for different lay-up sequences for 8 layered CFRP composite panel

Table 2.2: Lay-up sequences and corresponding critical buckling load

Lay-up sequence	Critical Buckling load in kN
$[0^\circ]_8$	1.03
$[45^\circ]_8$	1.55
$[90^\circ]_8$	1.03
$[(45^\circ/-45^\circ)_2]_s$	3.65
$[(90^\circ/0^\circ)_2]_s$	2.19
$[45^\circ/-45^\circ/90^\circ/0^\circ]_s$	3.55

Critical buckling load and load v/s out-of-plane/axial displacement behavior are analysed for various layup sequences (see Fig 2.5). All the lay-ups except 45 degree cross ply and quasi isotropic are having comparatively lesser critical buckling load (table 2.2). 45 degree cross ply is having a slightly higher critical buckling load as compared to quasi isotropic panel. But considering pre and post buckling stiffness, quasi isotropic is generally preferred. It is also better in terms of out-of-plane deflection behavior as well, whereas 45 degree cross ply is very less resistive towards bending once panel gets buckled. Although quasi isotropic lay-up is having the best buckling behaviour among all the lay-ups, it is observed that different quasi isotropic lay-up sequence is not showing similar buckling behavior in terms of critical buckling load and stiffness. For getting the best lay-up in terms of higher critical buckling loading and stiffness, a parametric study among different quasi isotropic lay-ups has been done as well and respective Load v/s end shortening behavior obtained is shown in the Fig 2.6.

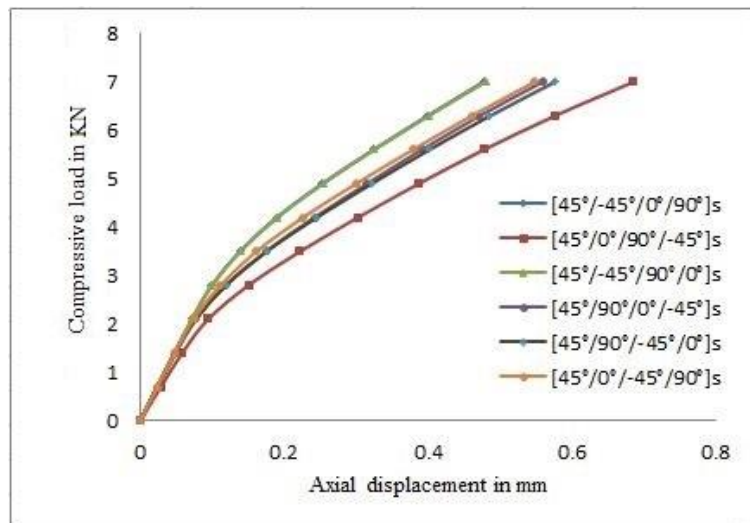


Fig 2.6: Load v/s end shortening behavior for various quasi isotropic lay-up sequences of 8 layered CFRP panel.

From Fig 2.6, quasi-isotropic $[45^\circ/-45^\circ/90^\circ/0^\circ]_s$ sequence is found out to be having maximum pre and post-buckling stiffness and higher critical buckling load. Therefore, same sequence has been considered for the further finite element as well as experimental study of 8 layered quasi isotropic panel. Similar optimization study has been carried out for CFRP panel with 16 layers and $[(45^\circ/-45^\circ)_2/(90^\circ/0^\circ)_2]_s$

sequence is found to be having the higher critical buckling load as well as post buckling stiffness.

2.4.2 Mode shapes

Mode shapes obtained from linear Eigen buckling analysis are plotted for UD ($[0^\circ]_8$) and quasi-isotropic ($[45^\circ/-45^\circ/90^\circ/0^\circ]_s$) CFRP panel. UD is showing single half sine wave along axial (loading) direction whereas quasi isotropic lay-up is showing double half sine waves (see Fig 2.7)

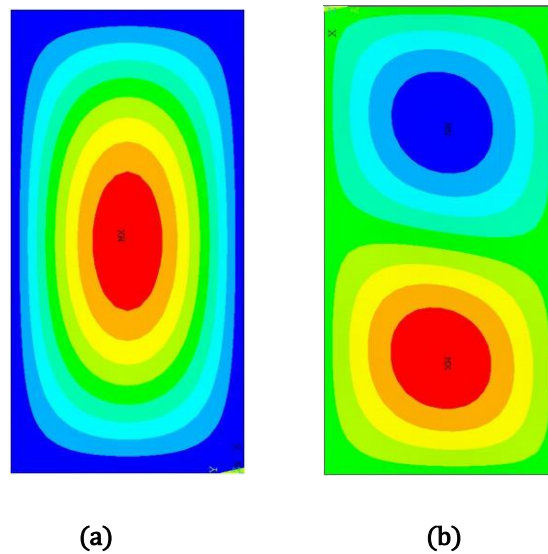


Fig 2.7: Mode shapes of CFRP composites under axial in-plane compressive loading from FEA (a) Unidirectional lay-up ($[0^\circ]_8$), $L_{cr} = 1.03$ kN (b) quasi isotropic lay-up ($[45^\circ/-45^\circ/90^\circ/0^\circ]_s$), $L_{cr} = 3.55$ kN.

First three buckling mode shapes of 16 layered CFRP quasi isotropic ($[(45^\circ/-45^\circ)_2/(90^\circ/0^\circ)_2]$) lay-up and corresponding critical buckling loads are given in Fig 2.8.

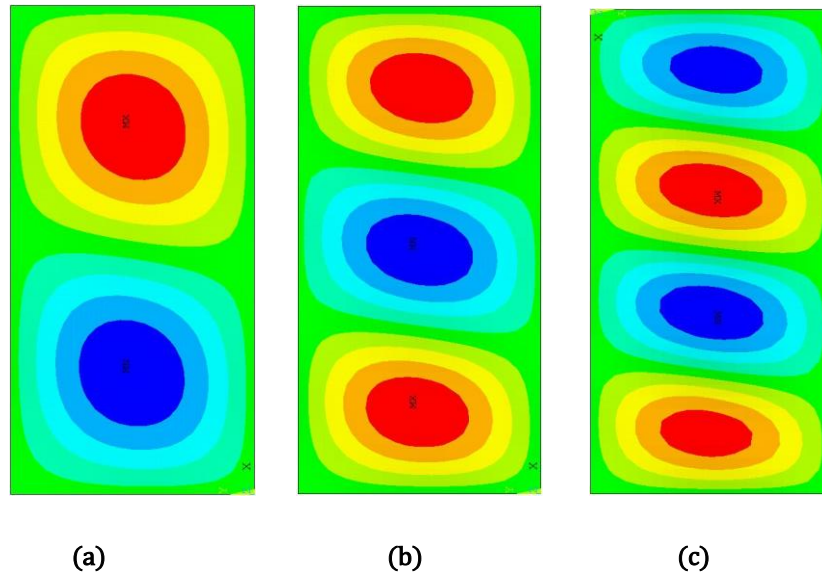


Fig.2.8: Different mode shapes for buckling of quasi-isotropic $([(45^\circ/-45^\circ)_2/(90^\circ/0^\circ)_2]_s)$ panel from finite element analysis (a) 1st Buckling mode shape, critical buckling load, $L_{cr} = 32.05$ kN (b) 2nd mode shape, $L_{cr} = 34.70$ kN (c) 3rd mode shape, $L_{cr} = 41.81$ kN.

2.4.3 Hole size study

A circular hole has been introduced at the center of quasi isotropic flat panel in the finite element model to observe the change in mode shape.

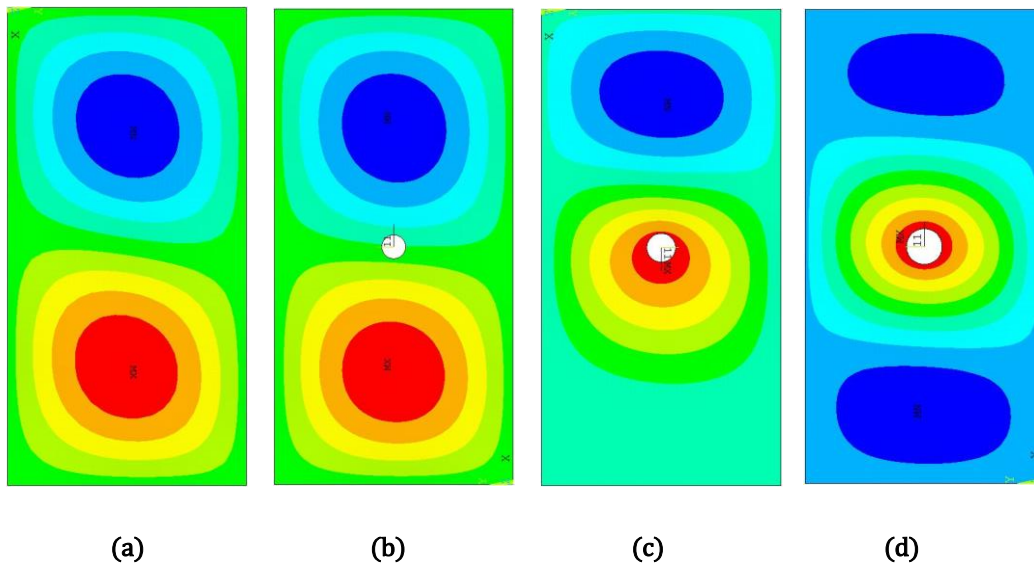
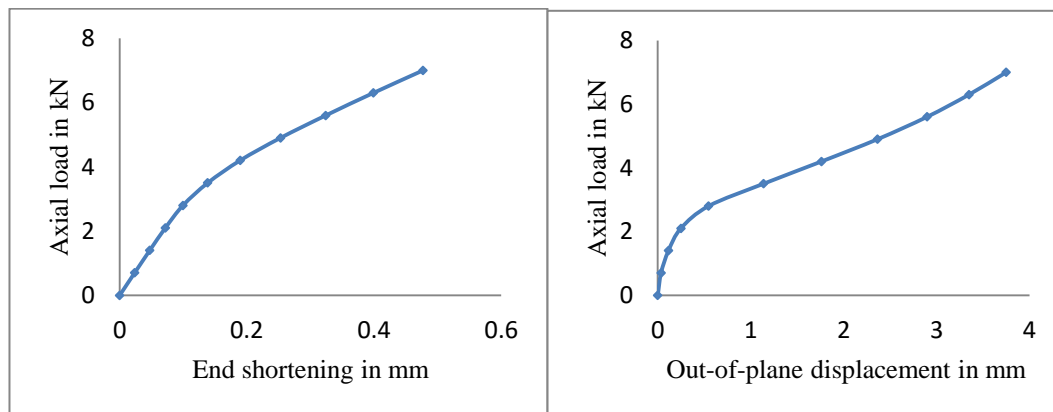


Fig.2.9: 1st buckling mode shapes of quasi-isotropic $([(45^\circ/-45^\circ)_2/(90^\circ/0^\circ)_2]_s)$ panel from finite element analysis (a) plate with no hole, critical buckling load, $L_{cr} = 32.05$ kN (b) plate with 20 mm diameter hole, $L_{cr} = 31.87$ kN (c) plate with 25 mm diameter hole, $L_{cr} = 31.63$ kN (d) plate with 30 mm diameter hole, $L_{cr} = 30.55$ kN.

First buckling mode shape has remained same for smaller hole diameter as compared the panel without hole. But, panel started showing different mode shapes as there is a significant increase in the hole size as shown in Fig. 2.9. Twenty mm hole in the middle did not cause any change in mode shape as compared to plate without hole though, there's a slight reduction in critical buckling load. When the diameter has increased to 25mm the maximum out-of-plane deflection of lower half sine wave has come up to hole region with smaller upper half sine wave. At 30 mm hole diameter, single half sine wave is projected with maximum out of plane deflection at center with 2 half sine waves on the top and bottom side with lesser amplitude. Another interesting thing to observe is, there is not much reduction in critical buckling load with increase in hole size because the natural pattern (mode shape) of the buckled wave is modified by the hole.

2.4.4 Post buckling results

First mode shape (see Fig. 2.7.b), scaled down by an imperfection factor has been used as the initial geometry for non-linear buckling analysis. All the further post buckling non-linear analyses are for the 1st buckling mode to validate the experimental results. End shortening and maximum out-of-plane deflection against load for 8 layered quasi isotropic $([45^\circ/-45^\circ/90^\circ/0^\circ]_s)$ panel is plotted to see the post buckling behaviour (Fig. 2.10).



(a)

(b)

Fig 2.10: Pre-buckling and post buckling behaviour from non-linear buckling analysis (a) End shortening with uniform compressive loading (b) Variation in maximum out-of-plane deflection with uniform compressive loading.

The Eigen buckling load for the panel is 3.55 kN, from load v/s axial displacement (end shortening) plot, it can be observed that after buckling, even though panel is able to carry further load, there is a significant reduction in the axial stiffness of the plate. In the initial pre buckling compression state, load is distributed uniformly through the plate width, but in the post buckling regime, when the panel got buckled, most of the load is carried by side edges, where there is no out-of-plane deflection and it is still under pure compression. That is why the panel is able to carry load even after buckling with a lesser stiffness. From out-of-plane deflection plot, we could see the drastic increase in slope in post buckling regime. Because once panel is perturbed from initial flat shape, lesser load is required to bend the panel further. Post buckling behaviour after introducing hole has been also analysed using FEA (see Fig 2.11).

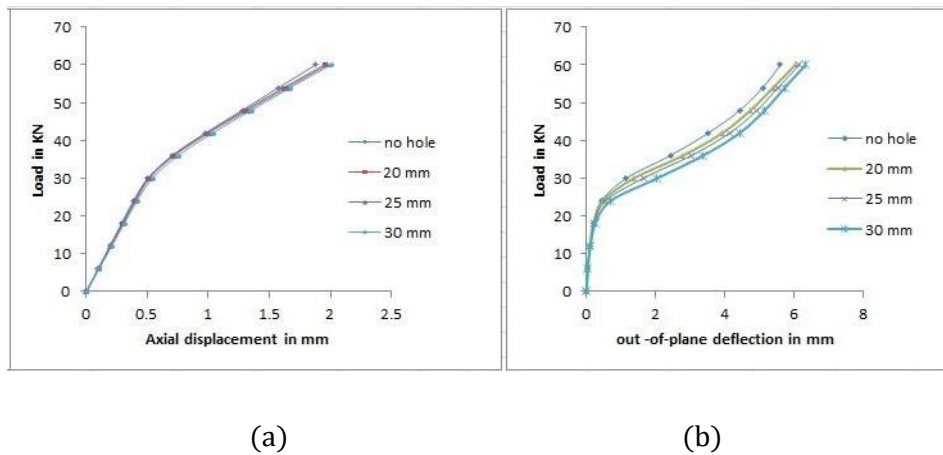


Fig 2.11: Pre-buckling and post buckling behaviour of panel with no hole and change in hole size from non-linear buckling analysis (a) End shortening with uniform compressive loading (b) Variation in maximum out-of-plane deflection with uniform compressive loading.

There isn't much change in stiffness with hole size as the diameter is very less (10 to 15 percentage) compared to the width of the panel. Considering the post buckling regime, hole in the middle of the panel does not affect the stiffness much since most of the load is carried by the side edges. Maximum out-of-plane deflection is slightly increases with the hole size.

2.5 Closure

Buckling behaviour of simply supported CFRP panel under axial compressive loading has been analysed numerically. Pre and post buckling behavior of end shortening and out-of-plane deflection are obtained by Eigen buckling followed by non-linear buckling

analysis. $[45^\circ/-45^\circ/90^\circ/0^\circ]_s$ sequence is having higher buckling load and post buckling stiffness as compared to UD and cross ply laminates and recommended for experimental studies. Hole with different sizes has been introduced into the middle of the panel and its effect on the buckling behavior is studied. Circular hole in the middle of the plate does not have an impact on critical buckling load as well as on pre and post buckling stiffness. But mode shape of the panel get influenced with increasing the hole diameter.

Chapter 3

Experimental studies

3.1 Introduction

Experimental tests are carried out for the better understanding of pre buckling and post buckling behaviour of CFRP composite panels with and without hole. Experimental study on 8 layered UD ($[0^\circ]_8$) and quasi isotropic ($[(45^\circ/-45^\circ/90^\circ/0^\circ)]_s$), 16 layered UD ($[0^\circ]_{16}$) and quasi isotropic($[(45^\circ/-45^\circ)_2/(90^\circ/0^\circ)_2]_s$) has been done using 3-D Digital Image Correlation (DIC) technique [25, 26] to determine the mode shape, in-plane stiffness, out-of-plane deflection and other buckling behaviors. 16 layered quasi isotropic ($[(45^\circ/-45^\circ)_2/(90^\circ/0^\circ)_2]_s$) panel with 30mm diameter hole has also been tested in experimental study [14, 17]. Panel are fabricated using hand lay-up assisted by vacuum bagging technique and testing is carried out using specially designed fixture to provide appropriate boundary condition and loading. 3D DIC is used for capturing whole field strain, axial displacement, out of plane displacement and mode shapes. Material characterisation test [30] based on ASTM standards [18] has been done to input the CFRP material properties into the FE simulation to ensure correlation with experimental results.

3.2 Material characterisation

Material characterisation on CFRP composite laminate has been carried out to obtain the material properties to input for the FE simulation and to ensure correlation with experimental results. For the current experimental study, unidirectional carbon fiber mat having a density of 200 grams per square meter is used as the reinforcement and CY-230 Epoxy resin mixed with HY-951 hardener in a weight-ratio of 10:1 [30] is used as the matrix for fabricating CFRP panels using vacuum bagging.

3.2.1 Specimen geometry and fabrication

All the testing specimens are casted as per the ASTM standards [18, 19], ASTM D-3039 for elastic moduli as well as Poisson's ratios and ASTM D-3518 for shear moduli. Specimen geometries are given in Fig 3.1.

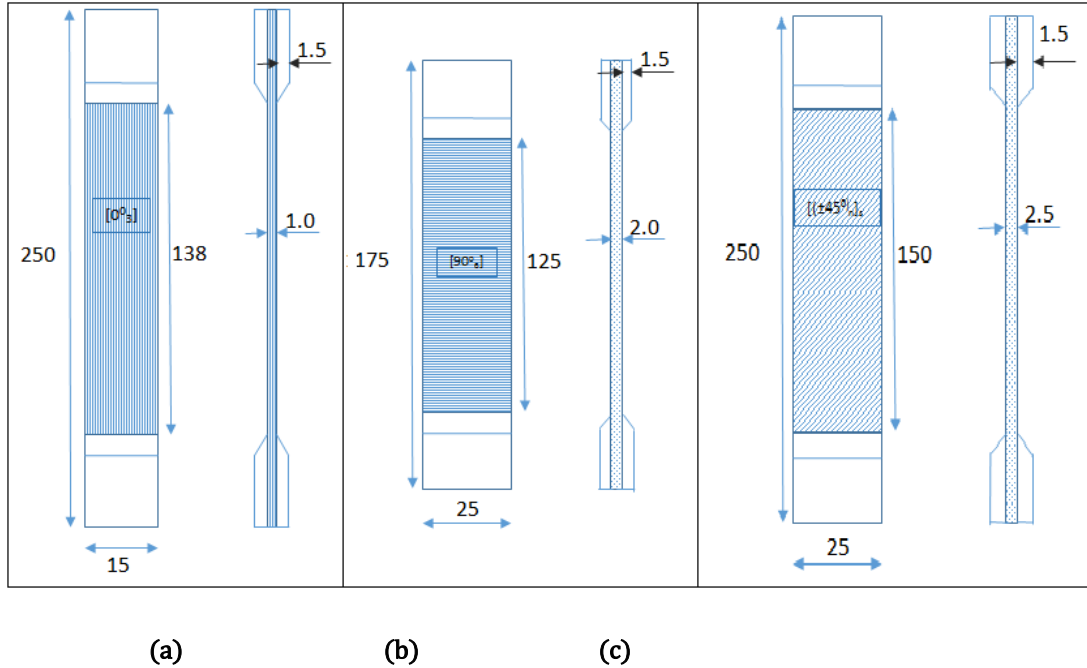


Fig 3.1: Specimen geometry and dimension for CFRP composite material characterisation (all dimensions are in mm) (a) for E_{11} and ν_{12} estimation [18] (b) for E_{22} estimation [18] (c) for G_{12} Estimation [19].

Specimens were fabricated as per the dimensions given in the Fig 3.1 using hand lay-up followed by vacuum bagging technique which gives an excellent fiber volume fraction. Unidirectional carbon fiber mat having a density of 200 grams per square meter is used as the reinforcement and CY-230 Epoxy resin mixed with HY-951 hardener in a weight-ratio of 10:1 is used as the matrix. Weight of resin taken is same as the weight of fiber to form laminate and then it is cured under vacuum for 24 hours. Aluminum coal plate of thickness 3 mm is placed on top to get uniform thickness throughout the specimen.

3.2.2 Test results are material properties

Material characterisation test has been carried out and then the results are extracted using extensometer as well as DIC.

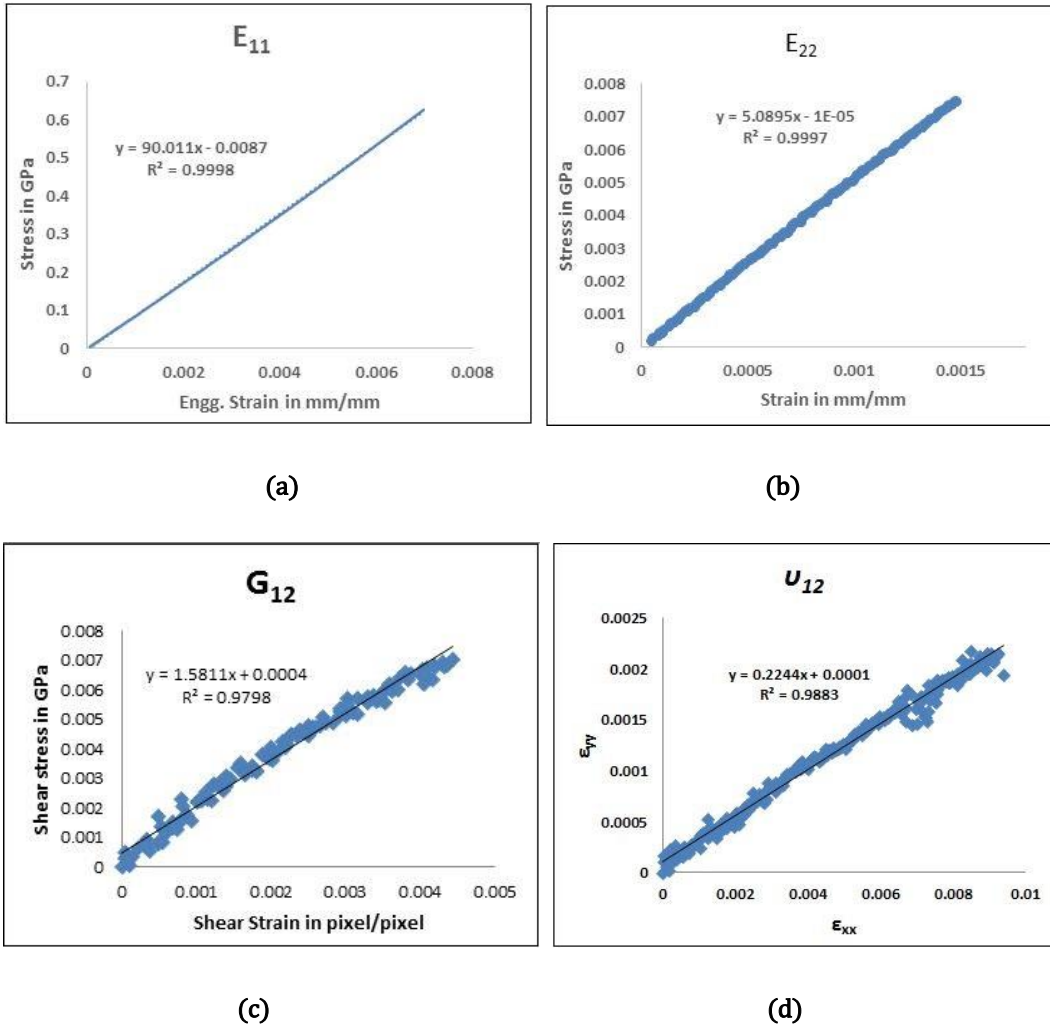


Fig 3.2: Graphs from experimental material characterisation tests to extract material properties (a) E_{11} estimation using stress strain curve from zero degree specimen (b) E_{22} estimation using stress strain curve from 90 degree specimen (c) ϑ_{12} estimation using longitudinal v/s transverse strain from zero degree specimen (d) G_{12} estimation using shear stress strain curve from 45 degree specimen.

E_{11} , E_{22} , ϑ_{12} and G_{12} are extracted directly from characterisation tests using the graphs shown in Fig 3.2. Other material properties are then obtained from theoretical formulation using the known material properties. To estimate ϑ_{23} ,

$$\vartheta_{23} = \vartheta_{12} \frac{1 - \vartheta_{21}}{1 - \vartheta_{12}}$$

Where,

$$\vartheta_{21} = \vartheta_{12} \frac{E_{22}}{E_{11}}$$

And to estimate out-of-plane shear property, G_{23}

$$G_{23} = \frac{E_{22}}{2(1 + \vartheta_{23})}$$

As CFRP composite used in the experiment are orthotropic in nature, E_{33} is same as E_{22} , ϑ_{13} is same as ϑ_{12} and G_{13} will be same as G_{12} . Ultimate longitudinal/transverse tensile strength and in-plane shear stress are also obtained from the experiment. All the mechanical properties obtained are listed in table 3.1 given below.

Table 3.1: Properties obtained from material characterisation

Material properties		Values
Longitudinal modulus	E_{11}	90.46 GPa
Transverse modulus	E_{22}	4.98 GPa
In-plane shear modulus	G_{12}	1.56 GPa
Out-plane shear modulus	G_{23}	1.91 GPa
In-plane Poisson's ratio	ϑ_{12}	0.2340
Out-plane Poisson's ratio	ϑ_{23}	0.3015
Longitudinal tensile strength	X_T	1049 MPa
In-plane tensile strength	Y_T	9.57 MPa
In-plane shear strength	S_{12}	13.77 MPa

3.2.3 Burn off test result

Burn-off test [22] has been carried out to determine the constituent content of CFRP made by hand lay-up assisted by vacuum bagging process. Burn-off test simply burns out the matrix by subjecting it to a very high temperature without affecting the fibers. Constituent mass fractions can be obtained by finding the masses of specimen before and after the test. Knowing the densities of constituents, individual volume fractions and void content can also be determined. Test has been carried out with the help of a muffle furnace, which is preheated to 500°C and crucibles along with sample is placed

in furnace and kept open using tong and then heated to 600°C at the rate of 5°C/min and is allowed to stay for 30 minutes at the same temperature. Then it is allowed to cool to room temperature slowly and then individual volume of fiber and matrix has found out by comparing weight of the fiber left out is with initial weight of the specimen using the individual densities. Estimated properties of CFRP composite is listed in the Table 3.2

Table 3.2: Properties obtained from burn off test

Properties	Values
Density	1.31 g/cm ³
Fiber mass fraction	60.2%
Fiber volume fraction	52.4%

3.3 Experimental buckling study

Experimental buckling studies carried out on CFRP laminated composites using 3-D DIC technique are discussed in this section.

3.3.1 Panel fabrication

Eight layered and 16 layered CFRP composite panels having a length of 400 mm and width of 200 mm were fabricated with unidirectional and quasi-isotropic lay-up sequences for the experimental studies. CFRP panels were fabricated using hand lay-up followed by vacuum bagging technique which gives an excellent fiber volume fraction. Unidirectional carbon fiber mat having a density of 200 grams per square meter is used as the reinforcement and CY-230 Epoxy resin mixed with HY-951 hardener in a weight-ratio of 10:1 is used as the matrix. Weight of the CY-230 Epoxy resin taken is same as the weight of fiber. Aluminum plate of thickness 3mm is placed on top to get uniform thickness throughout the panel and breather is used to absorb the excess resin. Panel is kept under vacuum for 24 hours after layup and then machined to the exact dimension. Steps of panel fabrication are given in the Fig 3.3 and machined panel with and without hole are shown in Fig 3.4.



(a)

(b)

(c)

(d)

Fig 3.3: Stages of panel Fabrication using hand lay-up followed by vacuum bagging technique (a) CFRP plies are stacked using matrix (b) breather sheet is placed over the CFRP plies (c) Aluminium plate is placed on top of breather (d) everything is covered with plastic cover and vacuum is applied.



(a)

(b)

(c)

(d)

Fig 3.4: 16 layered CFRP composite panels fabricated using hand lay-up followed by vacuum bagging technique (a) UD plate ($[0^\circ]_{16}$) (b) Quasi isotropic panel ($[(45^\circ/-45^\circ)_2/(90^\circ/0^\circ)_2]_s$) (c) Quasi isotropic ($[(45^\circ/-45^\circ)_2/(90^\circ/0^\circ)_2]_s$) panel with 30mm hole at the center (d) painted and speckled specimen for 3-D DIC.

3.3.2 Fixture design and fabrication

A fixture specially designed to realize the simply supported boundary condition and loading has been fabricated using EN-08 steel to perform the experiment. Fixture consists of 4 parts, bottom plate, top plate and 2 side supports. Side supports are bolted to bottom plate and can slide through the rectangular cut-out made on top plate. 60° V-grooves are made on inner surfaces of both plates and side supports to constrain out-of-plane deflection of all the sides of testing panel.

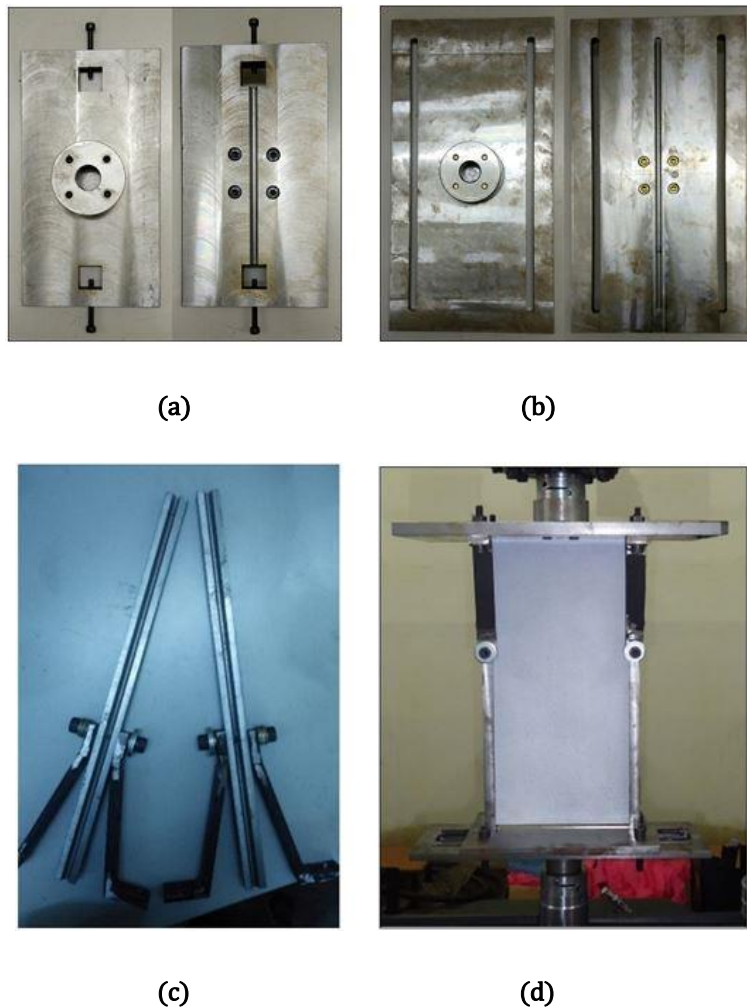


Fig 3.5: Fixture to provide simply supported boundary condition on all sides for buckling experiment (a) bottom plate (b) top plate (c) side supports (d) complete assembled fixture with buckling panel loaded.

As composite panels show high stiffness towards compression, it's very important to make sure that there isn't any kind of non parallelism between top and bottom plates. Non parallelism even in micro meter range could cause non uniform loading on the

panel, which results in getting wrong stiffness, mode shape and critical buckling load from the experiment.

3.3.3 Experimental setup

Eight and 16 layered CFRP panels with UD and quasi-isotropic lay-up sequences were tested using MTS servo-hydraulic cyclic testing machine of 100 kN capacity (Fig 3.6.1). Panels were speckle patterned with black and white dot paint (see Fig 3.4.d), after casting and machining for capturing images for 3-D DIC [31] analysis while testing [20]. Displacement controlled loading has been given to composite panels using the fixture at a rate of 0.4 mm per minute and images are simultaneously captured using two grasshopper CCD cameras (Point Grey-Grass-5055M-C) having a spatial resolution of 2448 x 2048 pixel at the rate of 2 images per second. Two white LED light sources have been used to provide better illumination over the panel surface. Images are captured using Vic snap software and post-processed is done using Vic 3-D software purchased from correlated solution. Testing setup has shown in Fig 3.6. A NI data acquisition card is used as an interface between image grabbing system and MTS controller system to record the load values for every image being captured.

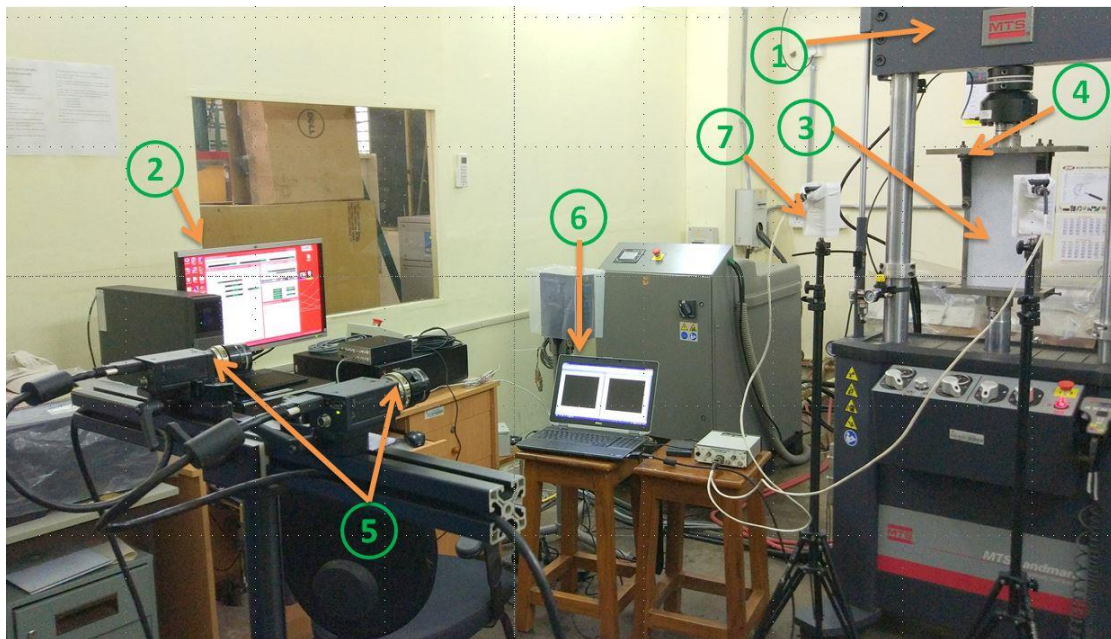


Fig 3.6: Experimental setup for buckling test of composite flat panels. (1) 100 kN MTS frame (2) User Interface (3) Plate under compression load (4) Fixture (5) CCD Cameras (6) Image grabbing PC (7) Light Source.

3.3.4 Post processing

2 grasshopper CCD cameras are used for measuring out-of-plane deflection and other parameters using binocular vision concept [21]. Three dimensional positioning of any point in the panel is possible with synchronized image grabbing using the 2 cameras positioned at same distance and calibrated. Post processing of images captured using 2 cameras has been done using Vic 3-D software. Complete surface of panel captured using camera is taken as region of interest (Fig 3.7), subset size is defined as 37×37 pixels and step size is taken 5 pixels per step.

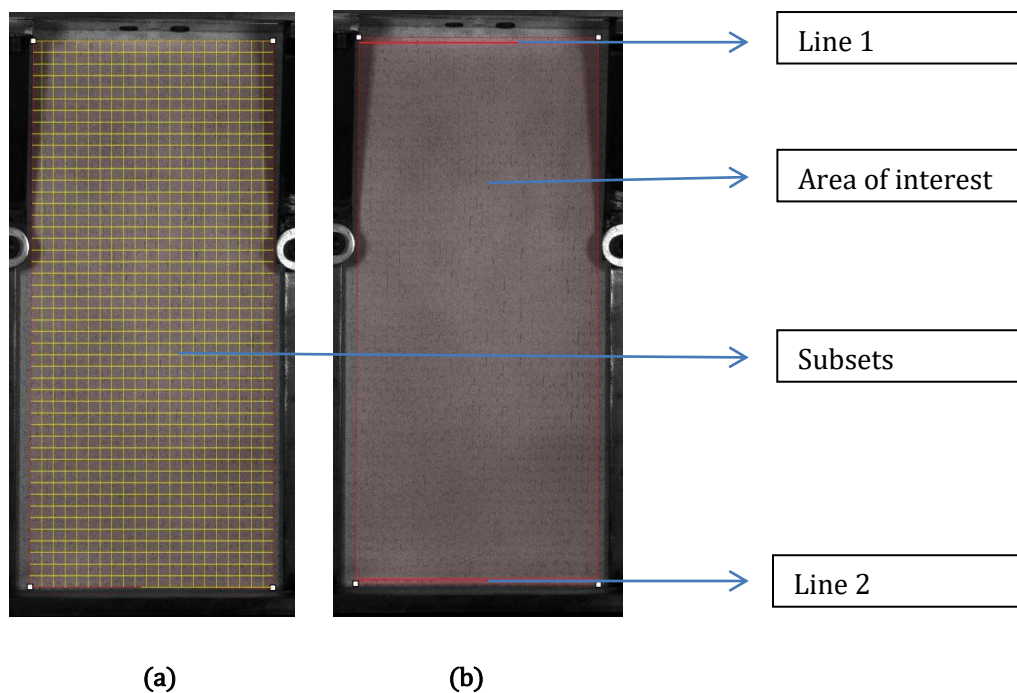


Fig 3.7: Speckled image of the panel captured by CCD camera for DIC post processing (a) subsets (b) Area of interest.

Displacement load is given to the panel from the bottom side with the help of fixture. Out-of-plane deflection with loading is obtained by extracting the maximum value of displacement along Z direction and end shortening is obtained by taking the difference between the average value of axial displacement along the lines 1 and 2 shown in Fig 3.7.

3.4 Result and discussion

After post processing all the experimental outcomes, the results have been compared with FEA results. Experimental pre buckling and post buckling results including mode shapes, axial displacement, out-of-plane deflection with load and panel failure for 8

layered UD ($[0^\circ]_8$), quasi isotropic ($[45^\circ/-45^\circ/90^\circ/0^\circ]_s$), 16 layered UD ($[0^\circ]_{16}$), quasi isotropic ($[(45^\circ/-45^\circ)_2/(90^\circ/0^\circ)_2]_s$) and 16 layered quasi isotropic ($[(45^\circ/-45^\circ)_2/(90^\circ/0^\circ)_2]_s$) with 30mm hole are discussed and compared with FEA in this section. Axial displacement contour for the panels while loading has been obtained from DIC to verify the uniform loading condition of the fixture and shown in Fig 3.8. The horizontal contour in the plot indicates the uniform loading condition. Relative displacement of top edge with respect to the bottom edge is showing a good match between FEA and experimental result with an error percentage less than 5%. So for the further axial displacement contour plots in this chapter, relative axial displacement is shown in the legend.

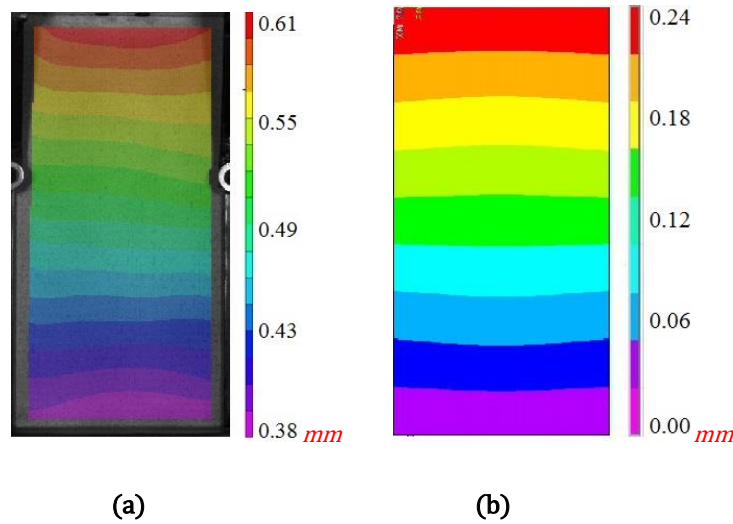


Fig 3.8: Finite element (FEA) and experimental (DIC) comparison of in plane axial displacement of 16 layered quasi isotropic ($[(45^\circ/-45^\circ)_2/(90^\circ/0^\circ)_2]_s$) CFRP panel at 15.0 kN load (a) DIC (b) FEA.

For experimental axial displacement from DIC, there is an axial displacement for the bottom side of the panel as well, which is supposed to have zero displacement. The reason for the axial displacement is because of the edge crushing of the panel while compressive loading as shown in Fig 3.9.

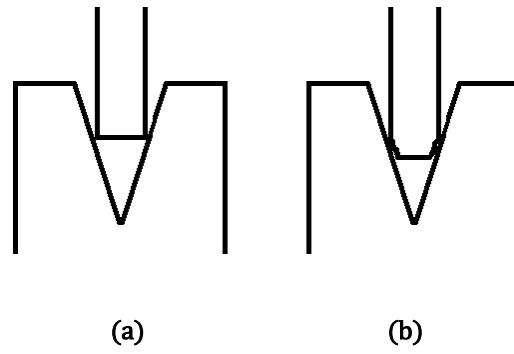


Fig. 3.9: Cross sectional view of bottom 'V' groove with panel (a) before loading (b) after loading.

To extract exact end shortening from the DIC average value relative displacement between line 1 and 2 (shown in Fig 3.7) has been calculated and then extrapolated to the complete length of the panel.



Fig 3.10: Axial displacement contour with axial displacement extracting lines.

$$\text{End shortening} = X_b - X_a$$

$$\frac{X_b - X_a}{ab} = \frac{X_{b1} - X_{a1}}{a_1 b_1}$$

$$\text{End shortening, } X_b - X_a = (X_{b1} - X_{a1}) \left(\frac{ab}{a_1 b_1} \right)$$

Where,

X_a, X_b, X_{b1}, X_{a1} are axial displacements at points a, b, a₁, b₁ respectively.

3.4.1 Mode shapes

Experimental mode shapes are extracted using 3-D DIC at a particular load and compared with FEA mode shapes at the same load in nonlinear buckling analysis. Mode shape comparison for 8 layered specimens is given in the Fig 3.11 and Fig 3.12.

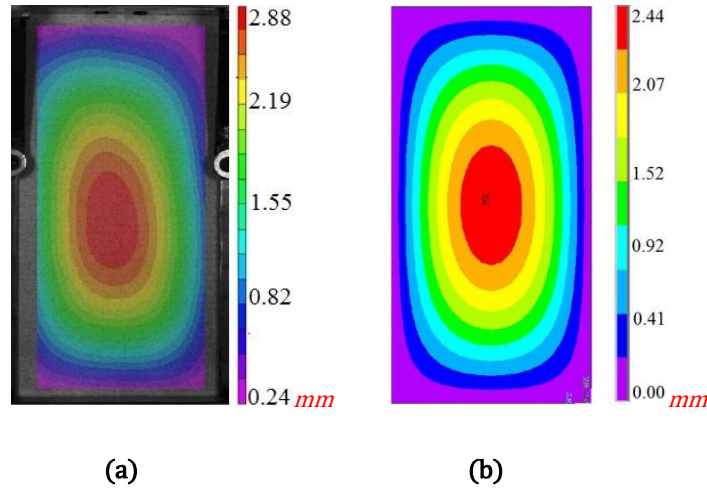


Fig 3.11: Finite element (FEA) and experimental (DIC) comparison of out-of-plane deflection of 8 layered UD ($[0^\circ]_8$) specimen at 2.0 kN load (a) DIC (b) FEA.

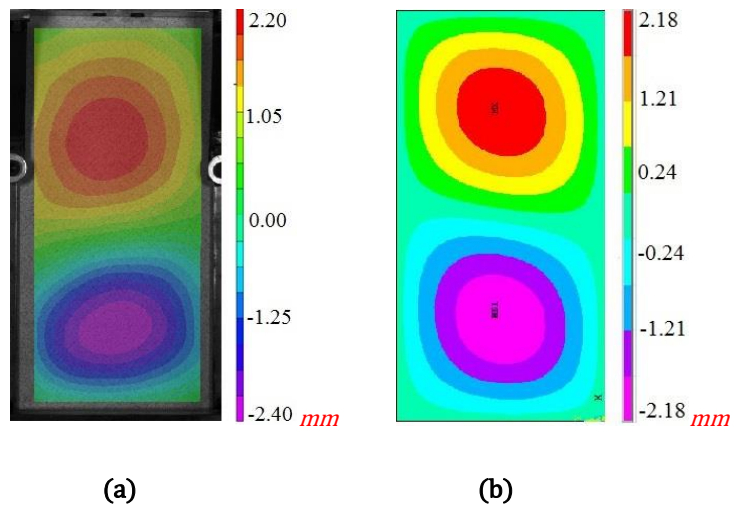


Fig 3.12: FEA and experimental (DIC) comparison of out-of-plane deflection of 8 layered quasi isotropic ($[45^\circ/-45^\circ/90^\circ/0^\circ]_8$) specimen at 4.5 kN load (a) DIC (b) FEA.

Complete area of panel could not be analysed using DIC as panel edges are going into the 'V' groove of the fixture and side supports are covering some space near the side

edges of the panel. Out-of-plane deflection is showing a good match (error percentage is less than 15%) between DIC and FEA for 8 layered specimens. Out-of-plane deflection contour comparison for 16 layered specimens is shown in Fig 3.13 and Fig 3.14.

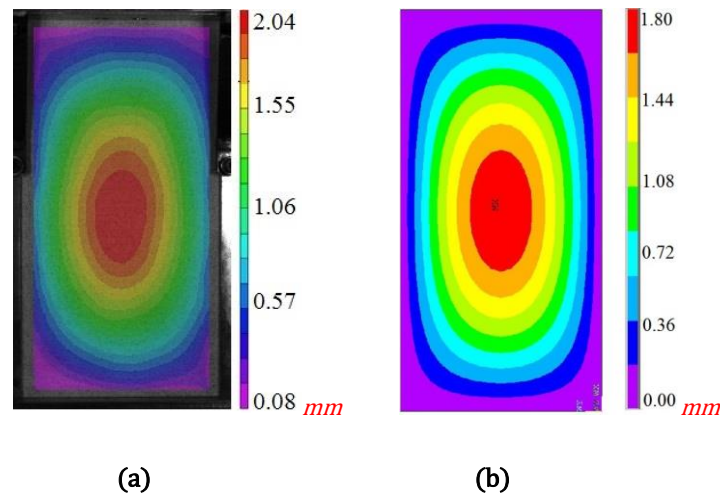


Fig 3.13: Finite element (FEA) and experimental (DIC) comparison of out-of-plane deflection of 16 layered UD $[(0^\circ)_{16}]$ specimen at 10.0 kN load (a) DIC (b) FEA.

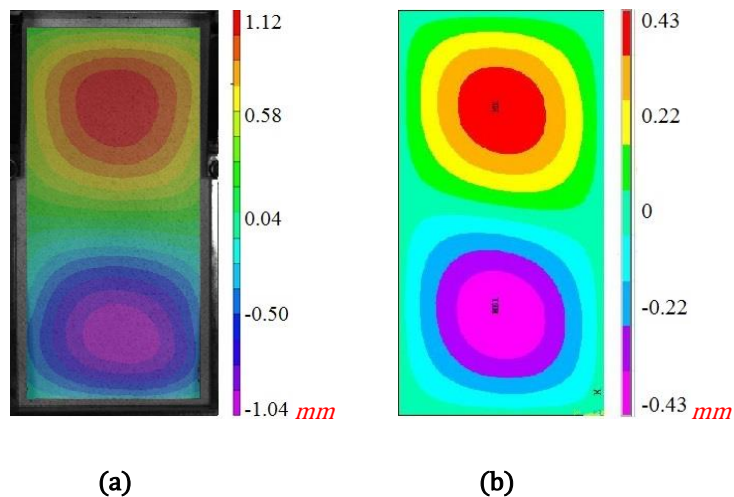


Fig 3.14: FEA and experimental (DIC) comparison of out-of-plane deflection of 16 layered quasi isotropic $[(45^\circ/-45^\circ)_2/(90^\circ/0^\circ)_2]_s$ specimen at 24.0 kN load (a) DIC (b) FEA.

In all the four cases experimental mode shape contours from DIC is closely matching with the FEA result. Maximum and minimum out-of-plane deflections are showing very good match in comparison except for 16 layered quasi isotropic $[(45^\circ/-45^\circ)_2/$

$(90^\circ/0^\circ)_2]_s$) specimen, where out-of-plane deflection from DIC is much higher than FEA. This is because the panel buckled at a lower load than predicted critical buckling load obtained from FEA. Mode shape for the panel with hole is given in Fig 3.15.

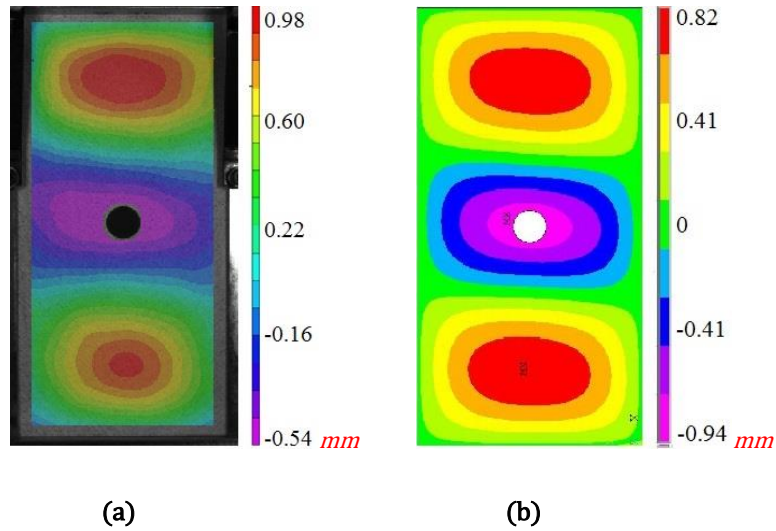
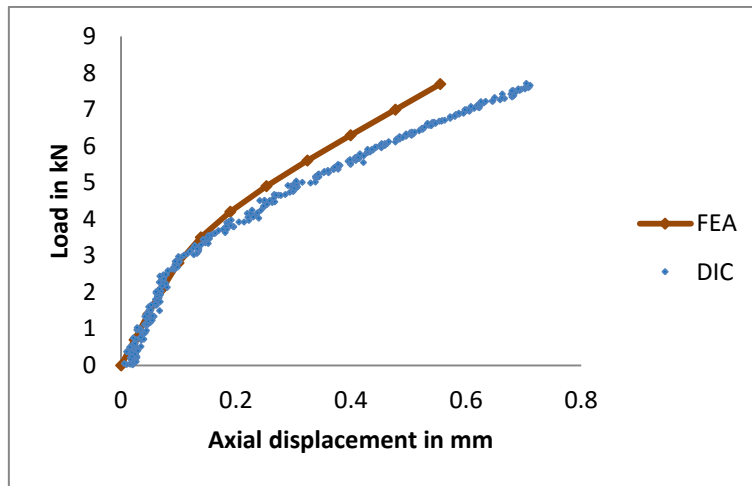


Fig 3.15: FEA and experimental (DIC) comparison of out-of-plane deflection of 16 layered quasi isotropic $[(45^\circ/-45^\circ)_2/(90^\circ/0^\circ)_2]_s$ panel with 30mm hole at 24 kN load (a) DIC (b) FEA.

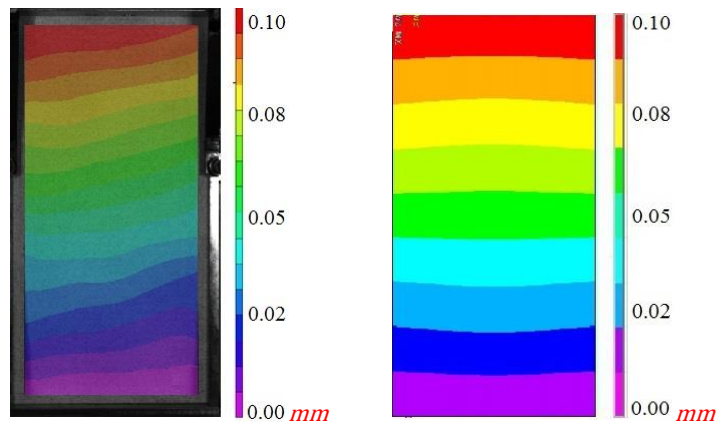
For panel with hole, experimental mode shape is comes out to be having 3 half sine waves along the axial direction as predicted by FEA and maximum deflection in the positive side is showing a good match with FEA, although a lesser deflection near hole has been observed in the DIC.

3.4.2 Axial and out-of-plane deflection

End shortening and out-of-plane deflection with loading are extracted from experiment using DIC to study the reduction of stiffness of the plate after buckling and also the out of plane displacement behaviour of the panels and then validated it with FEA predictions. Load v/s in plane and out-of-plane displacement plots for 8 layered panels is given in the Fig 3.16 and Fig 3.17.



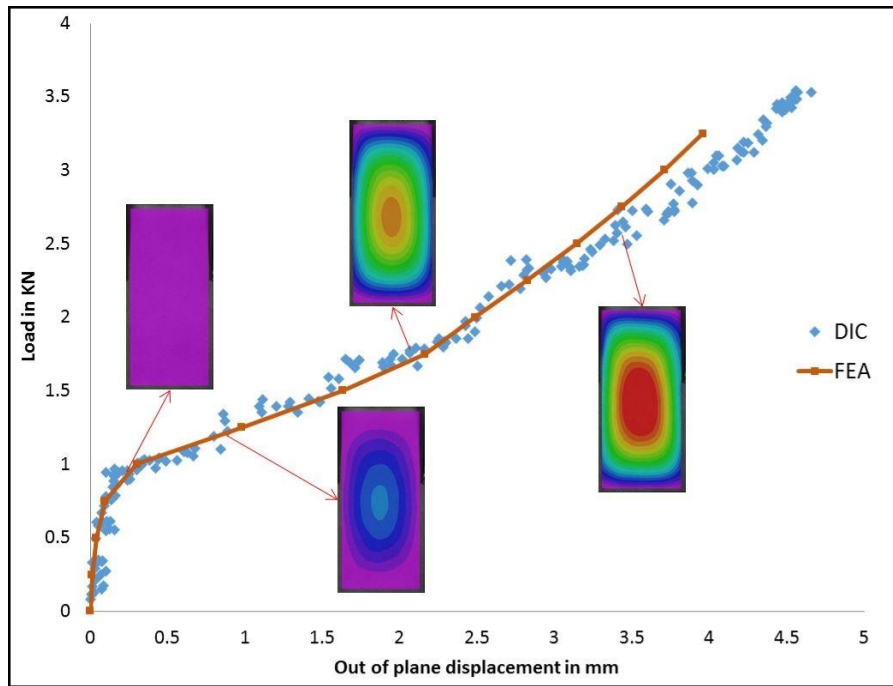
(a)



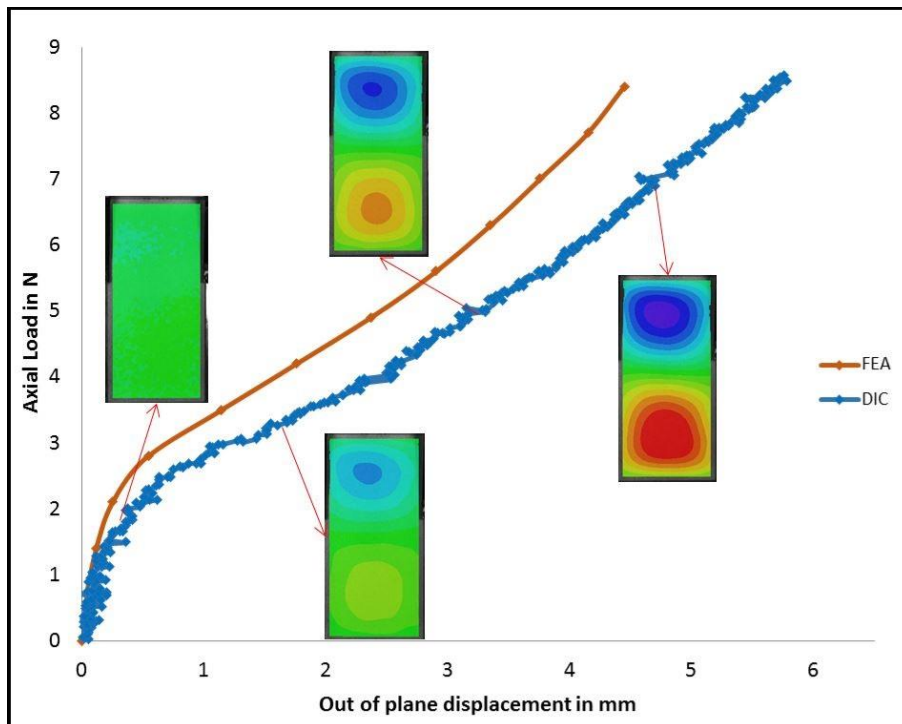
(b)

(c)

Fig 3.16: Experimental (DIC) and finite element (FEA) comparison of end shortening of quasi-isotropic $[45^\circ/-45^\circ/90^\circ/0^\circ]_s$ lay-up (a) load v/s end shortening graph for DIC and FEA (b) experimental in-plane axial displacement contour at 24 kN(c) FEA in-plane axial displacement contour at 24 kN.



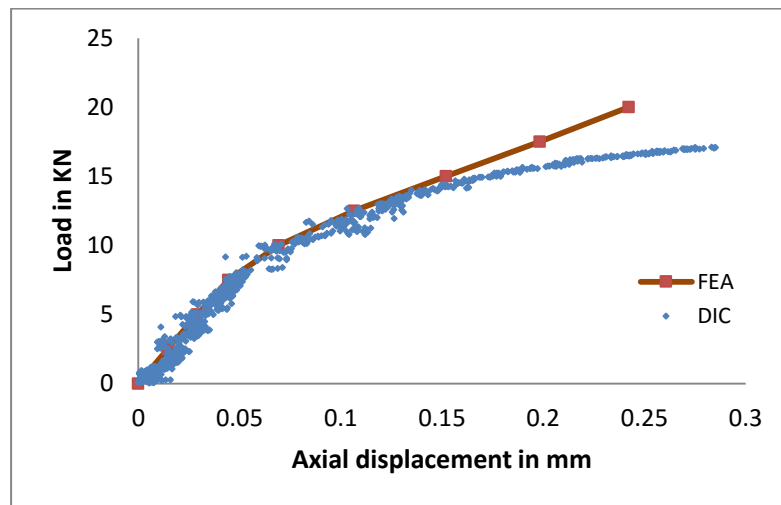
(a)



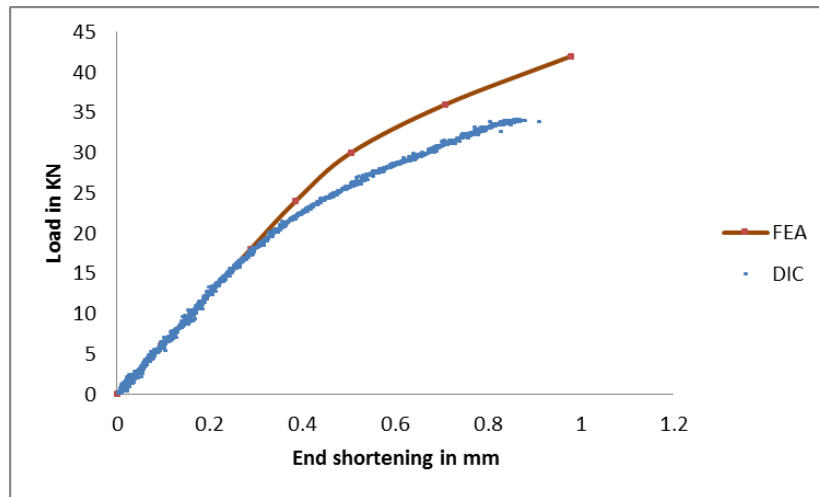
(b)

Fig 3.17: Experimental (DIC) and finite element (FEA) comparison of variation of out of plane deflection with loading (a) UD $[0^\circ]_8$ lay-up, (b) quasi-isotropic $[45^\circ/-45^\circ/90^\circ/0^\circ]_s$ lay-up.

For quasi isotropic panel, experimental pre buckling stiffness is closely matching with FEA, though there is a slight reduction in the post buckling stiffness (Fig 3.14.a). The axial displacement contour comparison between DIC and FEA at 24.0 KN is given in the Fig 3.14 b, c. There is a load sensitivity issue associated with testing machine for 8 layered UD panel compressions testing because of its high axial stiffness and lesser (nearly 1KN) critical buckling load. Problem has been solved by increasing the number of layers to 16 from 8. Considering load v/s out-of-plane deflection graph, as the slope changes gradually while panel the buckles, obtaining exact critical buckling load from experiment is impractical. Although a comparison can be done with FEA and relative change in critical buckling load can be determined. From Fig 3.17, for UD, the experimental critical buckling load is exactly same as FEA, whereas for quasi isotropic experimental critical buckling load is slightly less than the predicted load in FEA. Similar study has been then carried out using 16 layered CFRP composite panels with UD and quasi isotropic lay-up with and without hole. In plane and out-of-plane displacement plots are given in the Fig 3.18, Fig 3.19 and Fig 3.20.

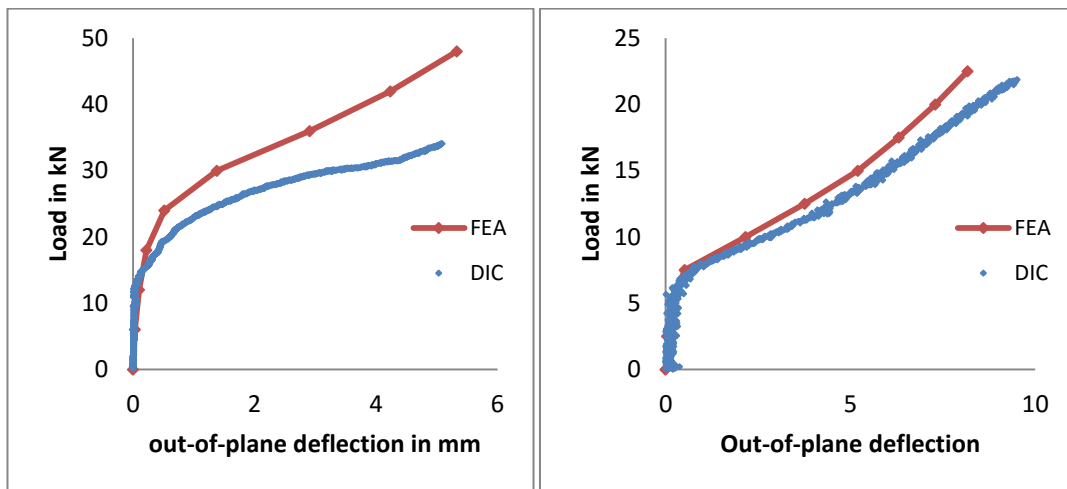


(a)



(b)

Fig 3.18: Experimental (DIC) and finite element (FEA) comparison of variation of in-plane axial displacement with loading for 16 layered panel (a) UD $[[0^\circ]_{16}]$ lay-up, (b) quasi-isotropic $[[45^\circ/-45^\circ]_2/(90^\circ/0^\circ)_{2s}]$ lay-up.



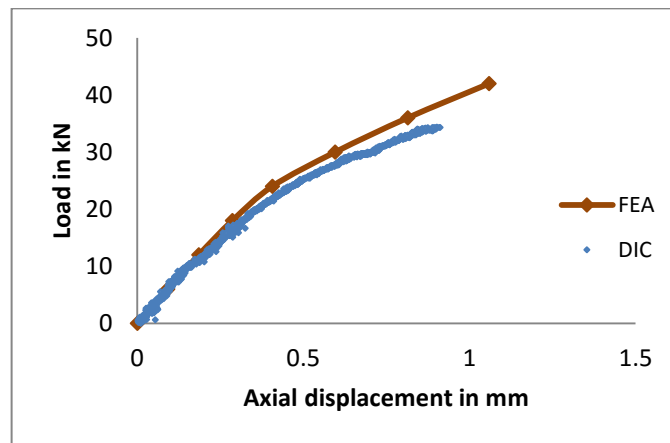
(a)

(b)

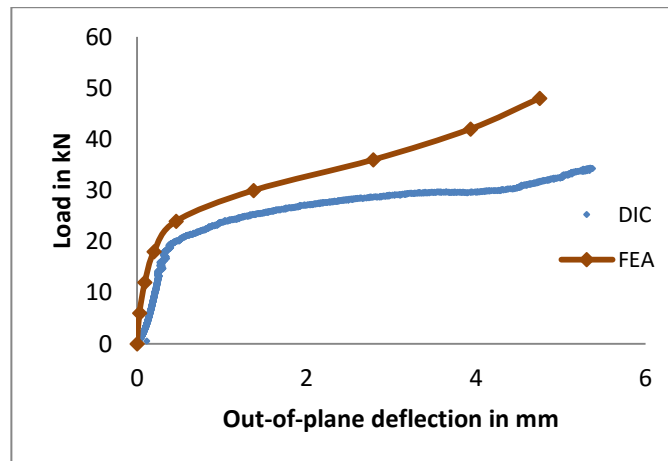
Fig 3.19: Experimental (DIC) and finite element (FEA) comparison of variation of out of plane deflection with loading for 16 layered panel (a) UD $[[0^\circ]_{16}]$ lay-up, (b) quasi-isotropic $[[45^\circ/-45^\circ]_2/(90^\circ/0^\circ)_{2s}]$ lay-up.

When number of layers increased from 8 to 16, significant changes can be observed in in-plane axial stiffness and critical buckling load. Critical buckling load has increased by a factor of 10 roughly, whereas in-plane axial stiffness has got doubled. From Fig 3.18 and Fig 3.19, all the experimental results are showing good agreement with FEA

results. For 16 layered UD specimen, partial damage has initiated at 15 kN and subsequently the stiffness got reduced (Fig 3.18.a). Quasi-isotropic panel has buckled at a lower load than predicted by FEA, so the out-of-plane deflection started increasing drastically at a lower load compared to FEA as shown in Fig 3.19.a. As the critical buckling load of the 16 layered panels is very high, there is a good chance that panel may get failed due to fiber compression just after buckling, which effectively leads into getting a lesser post buckling regime compared to 8 layered panels. So for the post buckling study 8 layered panels are more preferable.



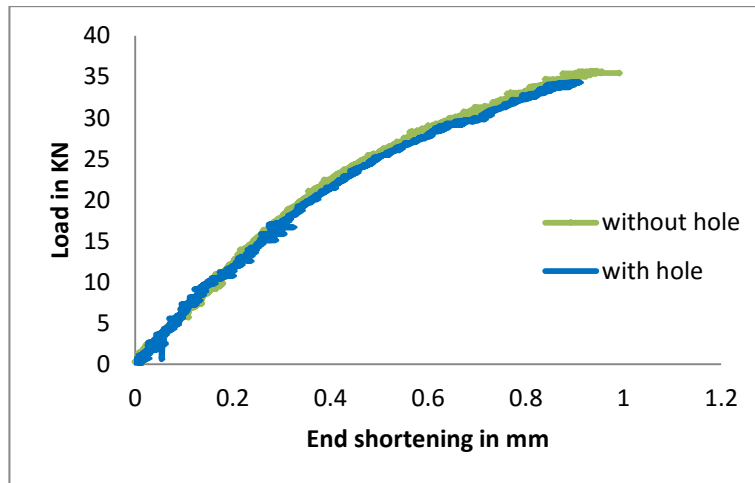
(a)



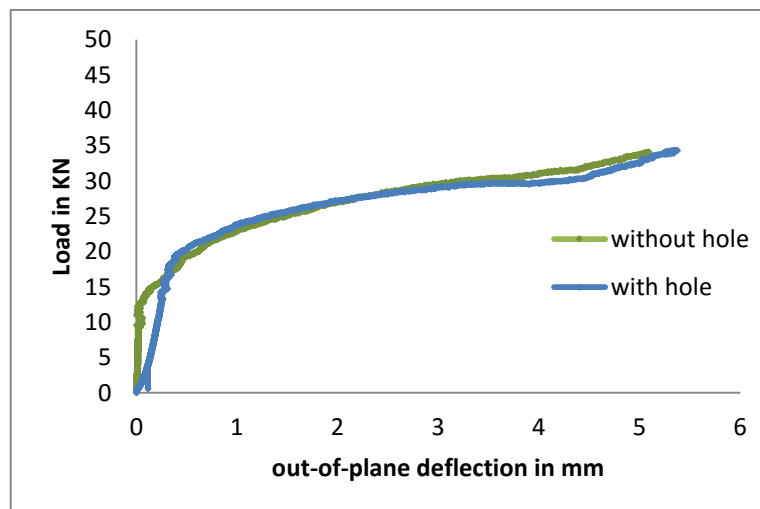
(b)

Fig 3.20: Experimental (DIC) and finite element (FEA) comparison for 16 layered quasi isotropic $[(45^\circ/-45^\circ)_2/(90^\circ/0^\circ)_2]_s$ plate with hole (a) end shortening v/s load (b) out-of-plane deflection v/s load.

Both in-plane and out-of-plane deflections for the panel with hole is showing good agreement with FEA results. However the experimental critical buckling load is slightly lower compared to FEA values. Panel could not carry much load after the buckling as there are 3 half sine waves in the mode shape (Fig 3.13). Half sine waves on the both ends are having higher out-of-plane deflections, which effectively cause the damage without allowing the plate to carry much further load after buckling.



(a)



(b)

Fig 3.21: Experimental in-plane and out-of-plane displacement with load comparison for 16 layered quasi isotropic $[(45^\circ/-45^\circ)_2/(90^\circ/0^\circ)_2]_s$ panel (a) plate without hole (b) plate with hole.

There is no much change in pre and post buckling stiffness after introducing hole in to the panel because most of the load is carried by side edges in post buckling regime as predicted by FEA. Critical buckling load has not been reduced much as the mode shape has got transformed to 3 axial half sine waves from plate's natural buckling mode shape after introducing the hole.

3.4.3 Failure mechanism

The damage mechanism from experiment has been obtained using DIC. The Fig 3.22 clearly shows that the failure has started from the top corners and progressed to the middle axis of the panel. DIC maximum strain contour (see Fig 3.23.a) also shows that the maximum compressive strain is near to the top corners which might have initiated the damage. Final damaged panel shown in Fig 3.23.b&c also shows a good agreement with the failure mechanism obtained from DIC. Similar mechanism has been observed with CFRP panel with 30 mm hole diameter (see Fig. 3.24).

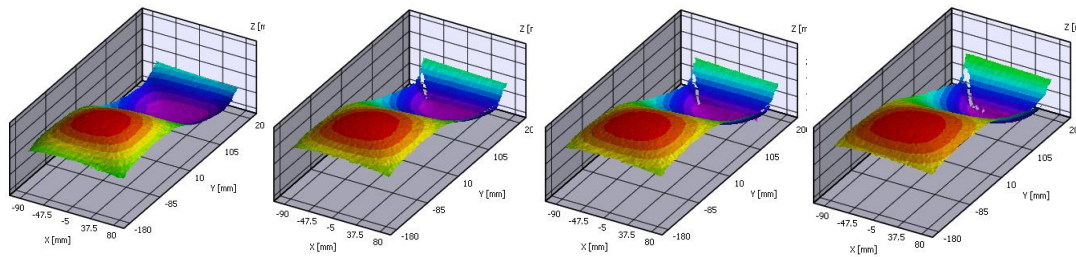
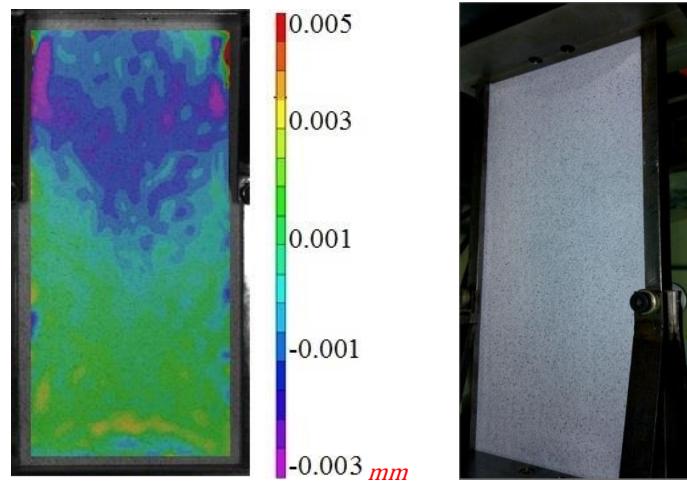
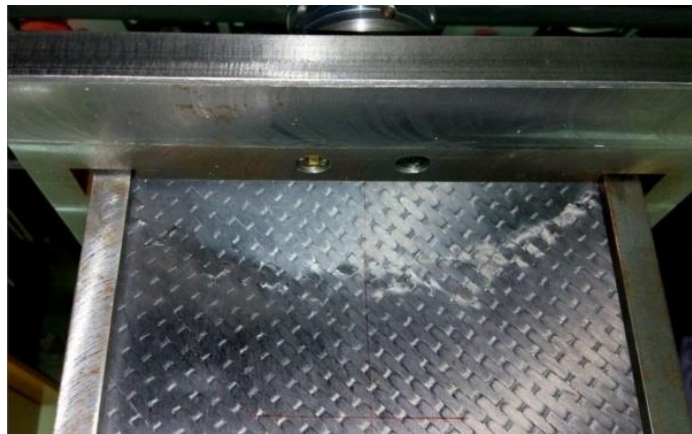


Fig 3.22: Failure propagation for 16 layered quasi isotropic panel from DIC.



(a)

(b)



(c)

Fig 3.23: Critical regions of failure for 16 layers quasi isotropic $[(45^\circ/-45^\circ)_2/(90^\circ/0^\circ)_2]_s$ panel (a) maximum principle strain contours from DIC (b) failed panel (c) closed view of failed region.

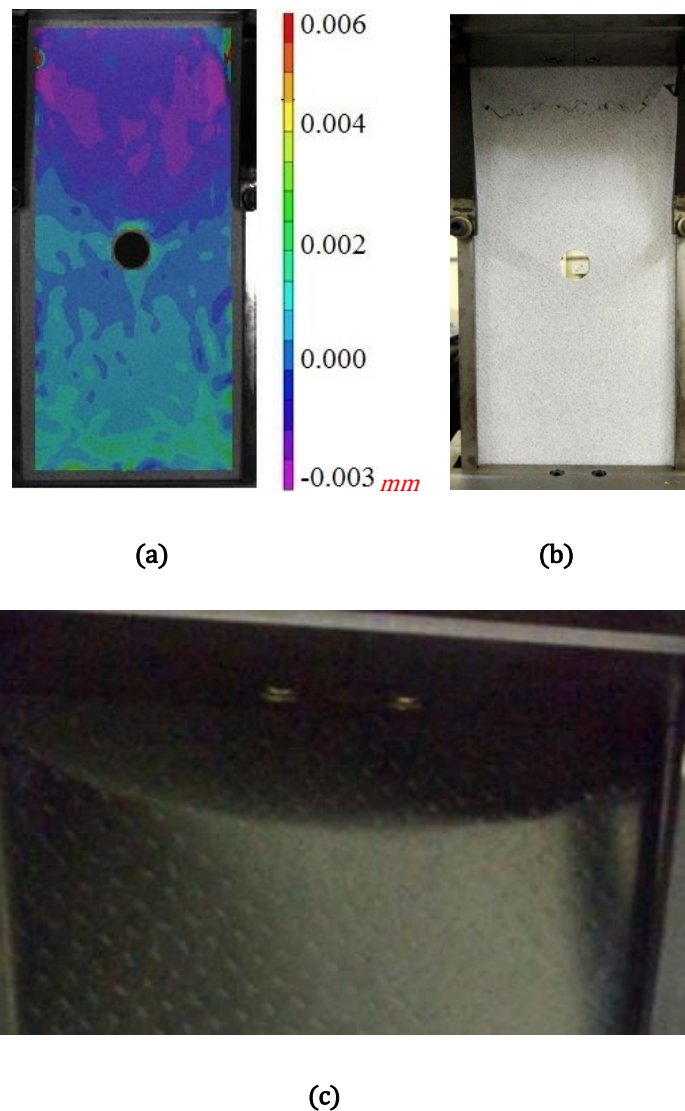


Fig 3.24: Critical regions of failure for 16 layers quasi isotropic $[(45^\circ/-45^\circ)_2/(90^\circ/0^\circ)_2]_s$ panel with hole (a) maximum principle strain contour from DIC (b) Failed panel (c) Closed view of failed region.

3.5 Closure

Experimental study on simply supported CFRP panel with and without hole under axial compressive loading using 3-D DIC technique has been described in this chapter. Panels were fabricated using hand lay-up assisted by vacuum bagging and then tested with the help of a specially designed fixture to provide proper boundary condition and uniform compressive loading. Whole field behaviour of panel under compressive loading is then studied using 3-D DIC and the results are then validated with finite element results. Fixture fabricated is able to provide the required boundary condition and uniform loading. 3D-DIC has been established as a proven technique on analyzing

the experimental buckling behavior. Damage mechanism from experiment has also been described with the help of DIC and it is observed that in both plate with and without hole, damage has initiated on top corners and progressed to the center. CFRP material characterisation has also been discussed in the chapter.

Chapter 4

Conclusion and recommendation for future work

4.1 Conclusion

Current study has been carried out for understanding the pre and post buckling behavior of the simply supported CFRP flat panel with and without hole under uniform in plane axial compressive loading. Finite element study using Eigen buckling followed by nonlinear analysis has been done to obtain the buckling behavior of CFRP panel including mode shapes, critical buckling load and axial/out-of-plane deflections, which are used to validate the experimental results obtained from 3-D DIC technique. Failure initiation has also been studied using Hashin's failure criteria in FEA and validated it with experimental results. From finite element study quasi isotropic lay-up shows the better post buckling stiffness and has got a higher critical buckling load compared to UD and cross ply lay-up sequences. And within the quasi isotropic lay-ups, $[45^\circ/-45^\circ/90^\circ/0^\circ]_s$ sequence is found out to be having the best buckling and post buckling behaviour. The 8 layered composite plate recommended for the experimental study of quasi isotropic panel is of the above sequence. Similar optimization study has been done with 16 layers and $[(45^\circ/-45^\circ)_2/(90^\circ/0^\circ)_2]_s$ sequence is found out be having the better pre and post buckling stiffness and higher critical buckling load. From experimental and finite element study, comparing UD and quasi isotropic lay-up sequences, even though the UD lay-up sequence is having a very high pre and post

buckling stiffness, the critical buckling load is very less compared to the quasi isotropic lay-up. Experimental mode shapes, critical buckling load and out-of-plane deflection are found out to be having an excellent match with the finite element result for both UD and quasi isotropic lay-up sequences. As the CFRP panel shows excellent stiffness towards compression, even slight non parallelism (in range of micro meters) between top and bottom side of fixture leads to experimental errors in terms of in plane axial stiffness. Making it parallel and perfectly aligning both the sides of the loading fixture could exert a uniform load and would generate exact stiffness and buckling mechanism in experimental studies. When number of layers is increased from 8 to 16, significant changes can be observed in in-plane axial stiffness and critical buckling load. Critical buckling load has increased by a factor of 10 roughly, whereas in-plane axial stiffness has got doubled. Introducing hole into the plate does not make much difference in buckling behavior of panel in terms of in-plane and out plane deflections, although it could affect the mode shape and failure mechanism of the composite panel. 3D-DIC has been established as a proven technique on analyzing the experimental buckling behavior as there is a very good coherence between FEA and DIC results.

4.2 Recommendation for future work

Current study has mainly focused on pre and post buckling behavior of CFRP laminated panel. Progressive damage modelling on FEA would give a deep insight of the failure mode and propagation in experimental study. Damage in the experiment can be detected by non-destructive testing and propagation can be evaluated using DIC. As the critical buckling load of the 16 layered panels is very high, there is a good chance that panel may get failed due to the fiber compression just after buckling, which effectively leads to a lesser post buckling regime compared to 8 layered panels. Therefore for the post buckling study 8 layered panels are more preferable. Even though introducing a single hole in the middle of the plate would not make much difference in buckling behavior, multiple holes and holes near side edges could make significant changes in in-plane and out-of-plane deflections in post buckling regime. Apart from circular holes, cutout with different shapes at different angle can also be investigated.

References

- [1] http://arch5541.wordpress.com/2013/01/08/the_great_metal_tube_in_the_sky.
- [2] Composite market report 2015: Market developments, trends, challenges and opportunities (Federation of reinforced plastics).
- [3] Chia, C.Y., Prabhakara, M.K., 1974. Post buckling behaviour of unsymmetrically layered anisotropic rectangular plates. *Journal of Applied Mechanics – Transactions of the ASME* 41, 155–162.
- [4] Harris, G.Z., 1975. The buckling and post-buckling behaviour of composite plates under biaxial loading. *International Journal of Mechanical Sciences* 17, 187–202.
- [5] Zhang Y, Mathews FL (1983) "Initial buckling of curved panels of generally layered composite materials" *Composite Structure*, 1, 3-30.
- [6] Zhang, Y., Matthews, F.L., 1985. Large deflection behavior of simply supported laminated panels under in-plane loading. *Journal of Applied Mechanics, ASME* 52, 553–558.
- [7] Michael P. Nemeth, Importance of Anisotropy on Buckling of Compression-Loaded Symmetric Composite Plates, *AIAA JOURNAL*, VOL. 24, NO. 11, 1986.
- [8] Tung, T. K., and Surdenas, J., 1987. Buckling of rectangular orthotropic plates under biaxial loading. *Journal of Composite Materials*, Vol. 21, pp.124-128.
- [9] Wang, H., Ou, M., Wang, T., 1991. Post-buckling behaviour of orthotropic rectangular plates. *Computers & Structures* 41 (1), 1–5.
- [10] Tuttle, M., Singhatanadgid P., and Hinds, G., 1999. Buckling of Composite Panels Subjected to Biaxial Loading. *Experimental Mechanics*, Vol. 39, pp.191-201.
- [11] Chainarin Pannok and Pairod Singhatanadgid. Buckling analysis of composite laminate rectangular and skew plates with various edge support conditions. - The 20th Conference of Mechanical Engineering Network of Thailand (2006)18-20.
- [12] Han Sung-Cheon, Lee Sang-Youl, Rus Guillermo, (2006) "Post buckling analysis of laminated composite plates subjected to the combination of in-

- plane shear, compression and lateral loading", *Int. J Solids Struct.*, 43 (18-19),5713-35.
- [13] Hongzhi zhong, Chao Gu; Buckling of symmetrical cross-ply composite rectangular plates under a linearly varying in-plane load. *Composite structures* 2007; 80; 42-48.
- [14] Cristopher Dennis Moen, Benjemin Schafer; Elastic buckling of thin plates with holes in compression or bending. *Thin-Walled Struct.* 2009; 47(12):1597-1607.
- [15] M. Aydin Komur a, Faruk Sen b; Buckling analysis of laminated composite plates with an elliptical/circular cutout using FEM; *Advances in Engineering Software* 2010; 41 (2010) 161–164.
- [16] Tamer Özben a, Nurettin Arslan; FEM analysis of laminated composite plate with rectangular hole and various elastic modulus under transverse loads; *Applied Mathematical Modelling* 34 (2010) 1746–1762.
- [17] A Lakshmi Narayan, Akrishn Amohana R; Buckling analysis of rectangular composite plates with rectangular cutout subjected to linearly varying in-plane loading using FEM; *Sadhana*; 2014, Volume 39, Issue 3, pp 583-596
- [18] ASTM-D 3039/D 3039M – 00, Standard Test Method for Tensile Properties of Polymer Matrix Composite Materials.
- [19] ASTM-D 3518/D3518M- Standard Test Method for In-Plane Shear Response of Polymer Matrix Composite Materials by Tensile Test of a 45° Laminate.
- [20] J. T. Ruan, F. Aymerich, J. W. Tong, and Z. Y. Wang, "Optical Evaluation on Delamination Buckling of Composite Laminate with Impact Damage," *Advances in Materials Science and Engineering*, vol. 2014, Article ID 390965, 9 pages, 2014. doi:10.1155/2014/390965.
- [21] Tailie Jina, 1, Ngoc San Haa, 1, Vinh Tung Lea and Nam Seo Gooa; Thermal buckling measurement of a laminated composite plate under a uniform temperature distribution using the digital image correlation method
- [22] ASTM D3171-15, Standard Test Methods for Constituent Content of Composite Materials.
- [23] H. Suemasu, T. Irie, and T. Ishikawa; Buckling and post buckling behavior of composite plates containing multiple delaminations, *Journal of Composite Materials*, vol. 43, no. 2, pp. 191–202, 2009.

- [24] H. Gu and A. Chattopadhyay; An experimental investigation of delamination buckling and post buckling of composite laminates, *Composites Science and Technology*, vol. 59, no. 6, pp. 903–910, 1999.
- [25] Chiara Bisagni and Carlos G. Dávila; xperimental investigation of the post buckling response and collapse of a single-stringer specimen, *Composite Structures*, Volume 108, February 2014, Pages 493–503.
- [26] J. T. Ruan, F. Aymerich, J. W. Tong and Z. Y. Wang³; Optical Evaluation on Delamination Buckling of Composite laminate with Impact Damage. Hindawi Publishing Corporation *Advances in Materials Science and Engineering* Volume 2014, 390965.
- [27] Robert M. Jones; *Mechanics of composite material*, Second edition
- [28] Ansys structural analysis 15.0, User guide.
- [29] Bathe, Klaus-Jürgen, and Eduardo N. Dvorkin. "A four-node plate bending element based on Mindlin/Reissner plate theory and a mixed interpolation." *International Journal for Numerical Methods in Engineering* 21.2 (1985): 367-383.
- [30] Kashfuddoja M, Prasath RGR and Ramji M. Study on Experimental Characterization of Carbon Fibre Reinforced Polymer Panel using Digital Image Correlation: A Sensitivity Analysis. *Optics and Lasers in Engineering*, 62, 17-30, 2014.
- [31] Naresh Reddy Kolanu, Suriya Prakash and Ramji M; Experimental study on compressive behavior of GFRP stiffened panels using digital image correlation. *Ocean engineering*, 114, 290-302,2016.